

1 **A novel tomato inter-specific (*Solanum lycopersicum* var. *cerasiforme*
2 and *S. pimpinellifolium*) MAGIC population facilitates trait association
3 and candidate gene discovery in untapped exotic germplasm**

4

5 **Andrea Arrones^{1†}, Oussama Antar^{1†}, Leandro Pereira-Dias¹, Andrea Solana¹, Paola
6 Ferrante², Giuseppe Aprea², Mariola Plazas¹, Jaime Prohens¹, María José Díez¹,
7 Giovanni Giuliano², Pietro Gramazio¹, Santiago Vilanova^{1*}**

8 ¹Instituto de Conservación y Mejora de la Agrodiversidad Valenciana, Universitat
9 Politécnica de València, Camino de Vera 14, 46022 Valencia, Spain

10 ²Agenzia Nazionale Per Le Nuove Tecnologie, L'energia e Lo Sviluppo Economico
11 Sostenibile (ENEA), Casaccia Research Centre, Rome, Italy

12 (anaroll@etsiamn.upv.es; oantar@doctor.upv.es; leapedia@upv.es; ansogar4@upv.es;
13 paola.ferrante@enea.it; giuseppe.aprea@enea.it; maplaav@upv.es; jprohens@upv.es;
14 mdiezni@upv.es; giovanni.giuliano@enea.it; piegra@upv.es; sanvina@upv.es)

15 [†]These authors have contributed equally to this work

16 *Corresponding author

17 **Abstract**

18 We developed a novel eight-way tomato multi-parental advanced generation inter-
19 cross (MAGIC) population to improve the accessibility of the genetic resources of tomato
20 relatives to geneticists and breeders. The inter-specific MAGIC population (ToMAGIC)
21 was obtained by inter-crossing four accessions each of *Solanum lycopersicum* var.
22 *cerasiforme* (SLC) and *S. pimpinellifolium* (SP), which respectively are the weedy
23 relative and the ancestor of cultivated tomato. The eight exotic ToMAGIC founders were
24 selected based on a representation of the genetic diversity and geographical distribution
25 of the two taxa. The resulting MAGIC population comprises 354 lines which were
26 genotyped using a new 12k tomato Single Primer Enrichment Technology (SPET) panel
27 and yielded 6,488 high-quality SNPs. The genotyping data revealed a high degree of
28 homozygosity (average 93.69%), an absence of genetic structure, and a balanced
29 representation (11.62% to 14.16%) of the founder genomes. To evaluate the potential of
30 the ToMAGIC population for tomato genetics and breeding, a proof-of-concept was
31 conducted by phenotyping it for fruit size, plant pigmentation, leaf morphology, and
32 earliness traits. Genome-wide association studies (GWAS) identified strong associations
33 for the studied traits, pinpointing both previously identified and novel candidate genes
34 near or within the linkage disequilibrium blocks. Domesticated alleles for fruit size were
35 recessive and were found, at low frequencies, in wild/ancestral populations. Our findings
36 demonstrate that the newly developed ToMAGIC population is a valuable resource for
37 genetic research in tomato, offering significant potential for identifying new genes that
38 govern key traits in tomato breeding. ToMAGIC lines displaying a pyramiding of traits
39 of interest could have direct applicability for integration into breeding pipelines providing
40 untapped variation for tomato breeding.

41 **Keywords:** tomato, *S. lycopersicum* var *cerasiforme*, *Solanum pimpinellifolium*, inter-
42 specific multi-parent advanced generation inter-cross (MAGIC), genome-wide
43 association studies (GWAS), fruit size, plant pigmentation, leaf morphology, earliness.

44

45 **Introduction**

46 Tomato (*Solanum lycopersicum* L.) is the most economically important vegetable
47 crop and a model plant species, with an extensive pool of genetic tools and resources. The
48 tomato research community has access to a wealth of genetic information for wild species,
49 landraces, and modern cultivars, including high-quality genome sequences (Rothan *et al.*,
50 2019). Several databases compiling genomic, genetic, transcriptomic, phenotypic, and
51 taxonomic information are available (Fei *et al.*, 2006, 2010; Bombarély *et al.*, 2010;
52 Suresh *et al.*, 2014; Kudo *et al.*, 2017). Over decades, several tomato bi-parental
53 populations have also been released including introgression lines (ILs), recombinant
54 inbred lines (RILs), advanced backcrosses (ABs), among others (e.g., Eshed and Zamir,
55 1995; Paran *et al.*, 1995; Tanksley and Nelson, 1996; Lippman *et al.*, 2007; Salinas *et al.*,
56 2013; Fulop *et al.*, 2016).

57 In the genomics era, new multi-parental populations have been developed
58 dramatically increasing mapping resolution (Scott *et al.*, 2020). Multi-parent advanced
59 generation inter-cross (MAGIC) populations are powerful next-generation pre-breeding
60 resources with increased diversity and high recombination rates, suitable for QTL
61 mapping and candidate gene identification (Mackay and Powell, 2007; Cavanagh *et al.*,
62 2008; Arrones *et al.*, 2020; Scott *et al.*, 2020). In tomato, only two MAGIC populations
63 have previously been released. The first one was a MAGIC population developed by
64 crossing four large-fruited *S. lycopersicum* accessions with four cherry-type accessions
65 of *S. l. var. cerasiforme* (Pascual *et al.*, 2015). Final lines were used to study fruit weight
66 distribution in the population in different environments, identifying QTLs that
67 colocalized with already cloned genes. Subsequently, Campanelli *et al.* (2019) developed
68 a MAGIC population that included seven cultivated accessions of tomato and one of the
69 wild *S. cheesmaniae* as founders. The *S. cheesmaniae* accession was selected for its biotic
70 and abiotic stress tolerance, yield and resiliency (Nesbitt and Tanskley, 2002).

71 The development of MAGIC populations using wild species as founders represents
72 a promising way to combine the potential of these experimental populations for QTL/gene
73 mapping together with the exploitation of the large phenotypic and genetic variation from
74 the wild donor introgressions. Here, we present a novel eight-way inter-specific tomato
75 MAGIC population (ToMAGIC) obtained by using *S. l. var. cerasiforme* (SLC) and *S. pimpinellifolium* (SP)
76 accessions as founders, which respectively are the closest relative and the ancestor of cultivated tomato (Peralta *et al.*, 2008). Cultivated tomato suffered
77 strong genetic bottlenecks during domestication and breeding processes, resulting in low
78 genetic diversity of tomato landraces and heirlooms (Blanca *et al.*, 2015). Based on
79 previous morphological characterization and resequencing data availability, the eight
80 selected founders of the new ToMAGIC population represent a wide genetic and
81 morphological variation, as well as differences in ecological adaptation (Blanca *et al.*,
82 2015; Gramazio *et al.*, 2020a). Founders are very diverse in terms of fruit, vegetative, and
83 flowering traits but also their capacity of adaptation to different conditions, ranging from
84 desert to tropical forest environments, and from sea level to over 1,500 m altitude.
85 Therefore, one of the aims of this population is to recover Andean variability lost during
86 the domestication process, by using a substantial proportion of the fully cross-compatible
87 weedy and wild tomato diversity.

89 This ToMAGIC population may have a large potential to identify new genomic
90 regions and candidate genes of interest in breeding, as well as to validate genes and QTLs
91 already described in a genetic background other than that of cultivated tomato. In this
92 way, another aim of this population is dissecting the control of different traits, including
93 those involved in the early domestication of tomato (Frary and Doganlar, 2003). The
94 introduction of exotic germplasm will be useful for shedding light on the genetics of
95 agronomic and adaptation traits present in these materials, as well as for the selection of
96 elite lines of interest for tomato breeding (Arrones *et al.*, 2020). In our work, the
97 integration of high-throughput genotyping of the recombinant ToMAGIC population
98 together with the phenotyping of specific traits across different plant parts has effectively
99 demonstrated a proof-of-concept for the high-precision fine mapping of these traits. This
100 approach has not only validated previously identified candidate genes for the traits studied
101 in a SLC and SP genetic background, but also led to the discovery of new candidate genes,
102 and the observation of additional phenotypic-causing variants, underscoring the great
103 potential of the ToMAGIC population for tomato genetics and breeding.

104

105 **Materials and methods**

106 **ToMAGIC founders**

107 The inter-specific tomato MAGIC (ToMAGIC) population was developed through
108 the inter-crossing of SLC and SP accessions. Founders consist of four weedy *S. l.* var.
109 *cerasiforme*, i.e., BGV007931 (SLC1), LA2251 (SLC2), PI487625 (SLC3), and
110 BGV006769 (SLC4), and four wild *S. pimpinellifolium*, i.e., BGV007145 (SP1),
111 BGV006454 (SP2), BGV015382 (SP3), and BGV013720 (SP4). Their geographical
112 origin, including geographical coordinates and altitude, and environmental parameters
113 (Mean temperature, temperature range, precipitation, etc.) are known (Martínez-Cuenca
114 *et al.*, 2020). With respect to the Heinz 1706 SL4.0 reference genome (Hosmani *et al.*,
115 2019), the total variants identified in SLC accessions ranged from 1.2 million in SLC2 to
116 1.9 million in SLC1, while in the SP accessions, they ranged from 3.1 million in SP4 to
117 4.8 million in SP3 (Gramazio *et al.*, 2020a). This set of variants was over 1,600-fold more
118 abundant than the one used in the previous study of Blanca *et al.* (2015), where the eight
119 founders were also genotyped.

120 **ToMAGIC population development**

121 Although low heterozygosity levels were observed for founders in previous studies
122 (Blanca *et al.*, 2015), before starting with the ToMAGIC population cross-design, two
123 generations of selfing of the founders were performed to ensure high homozygosity. To
124 develop the ToMAGIC population, founder lines were inter-crossed by following a
125 “funnel” approach including two extra generations of inter-crosses among the offspring
126 of the double hybrid crosses. These extra steps were performed to increase recombination
127 events among the genomes of the eight founders during the population development to
128 achieve better mapping and QTL identification resolution (Arrones *et al.*, 2020). The first
129 step in developing the MAGIC population consistent in crossing the SLC parents with
130 the SP ones to produce interspecific F₁ hybrids (SLC1 × SP2, SLC2 × SP1, SLC3 × SP4,
131 and SLC4 × SP3). These F₁ hybrids were subsequently inter-crossed in pairs (SLC1 ×

132 SP2 with SLC2 × SP1, and SLC3 × SP4 with SLC4 × SP3) directly (') and reciprocally
133 (") to obtain four genetically segregating double hybrids (DHY1', DHY1'', DHY2', and
134 DHY2''). In this way, genomes from both species were mixed since the beginning of the
135 development of the MAGIC population. Then, DHY1' or DHY1'' individuals were
136 crossed with DHY2' or DHY2'' individuals obtaining a set of materials coming from the
137 first inter-cross generation (IC1), which were an admixture of the genomes of the eight
138 founders. DHYs were crossed by following a chain pollination scheme, where each
139 individual was used as a female and male parent of different crosses (Díez *et al.*, 2002;
140 Mangino *et al.*, 2022). In the same way, individuals from the second inter-cross (IC2)
141 generation were also inter-crossed following a chain pollination scheme. This step was
142 repeated to obtain the individuals from the third inter-cross generation (IC3). Finally,
143 progenies of the IC3 were selfed for five generations by single seed descent (SSD) to
144 obtain the ToMAGIC recombinant inbred lines. To accelerate the obtention of the SSD
145 generations, selfings were stimulated by mechanical vibration and pruning was done
146 manually, regulating vegetative growth and flowering. A set of 354 ToMAGIC lines were
147 used in this study for phenotyping and genotyping.

148 Seeds from the 354 ToMAGIC lines were germinated in seedling trays with Humin-
149 substrat N3 substrate (Klasmann-Deilmann, Germany) in a climatic chamber under a
150 photoperiod and temperature regime of 16 h light (25 °C) and 8 h dark (18 °C). Plantlets
151 were subsequently transplanted to individual thermoformed pots (1.3 l capacity) for
152 acclimatisation and grown in a pollinator-free glasshouse of the Universitat Politècnica
153 de València (UPV, Valencia, Spain). Plants were fertirrigated using a drip irrigation
154 system and trained with vertical strings. Phytosanitary treatments against whiteflies and
155 *Tuta absoluta* were performed when necessary.

156 ***High-throughput genotyping***

157 Young leaf tissue was sampled from the 354 ToMAGIC lines. Genomic DNA was
158 extracted using the SILEX extraction method (Vilanova *et al.*, 2020). DNA quality and
159 integrity were checked by agarose electrophoresis and NanoDrop ratios (260/280 and
160 260/230), while its concentration was estimated using a fluorescent DNA intercalating
161 agent (e.g., Quant-iT PicoGreen dsDNA Assay Kit, Thermo Fisher Cat. No. P7589) and
162 a microplate reader (Thermo Fisher Scientific). Samples were sent to IGATech company
163 (Udine, Italy) for library preparation and sequencing (150 paired-end) for a high-
164 throughput genotyping using a newly developed 12k probes tomato Single Primer
165 Enrichment Technology (SPET) panel, which is considerably improved over the original
166 5k probes tomato set (Barchi *et al.*, 2019). The new SPET panel comprises 12,000 probes
167 and was developed by selecting the most informative and reliable polymorphisms (of
168 which ~11,500 within 100 nt of a gene and ~500 in intergenic regions) (Aprea *et al.*, in
169 preparation).

170 Cleaning of raw reads was performed using Fastp (Chen, 2023). Clean reads were
171 mapped onto the tomato reference genome Heinz 1706 SL4.0 (Hosmani *et al.*, 2019)
172 using BWA-MEM (Li, 2013) with default parameters; finally, GATK was used for
173 variant calling (DePristo *et al.*, 2011), following the best practices recommended by the
174 Broad Institute. The SNPs identified by the tomato SPET panel were first filtered by
175 coverage ≥ 10 and quality GQ ≥ 20 using bcftools

176 (<https://doi.org/10.1093/gigascience/giab008>), and then filtered using the TASSEL
177 software (ver. 5.0, Bradbury *et al.*, 2007) to retain the most reliable ones (minor allele
178 frequency > 0.01, missing data < 0.1, and maximum marker heterozygosity < 0.7). In
179 addition, a linkage disequilibrium (LD) k-nearest neighbour genotype imputation method
180 (LD KNNi) was performed to fill the missing calls or genotyping gaps (Troyanskaya *et*
181 *al.*, 2001). Final marker density along chromosomes was represented using the R package
182 chromPlot (Oróstica and Verdugo, 2016).

183 ***Population diversity analysis***

184 A principal component analysis (PCA) was performed to assess the population
185 structure of the MAGIC population. PCA scores were generated in TASSEL software
186 (ver. 5.0, Bradbury *et al.*, 2007). For graphically plotting the final PCA results the R
187 package ggplot2 was used (Wickham, 2016). A heat map of the kinship matrix to identify
188 possible relationships between lines was generated with GAPIT software (v.3, Wang and
189 Zhang, 2021). A dendrogram of the MAGIC population was generated using the
190 neighbor-joining method (Saitou and Nei, 1987) and the graphical representation was
191 displayed and edited using the iTOL v.4 software (Letunic and Bork, 2019) to evaluate
192 the genetic similarities among ToMAGIC lines and founders. Parental contribution to the
193 ToMAGIC lines and haplotype blocks was estimated by using the R package
194 HaploBlocker (Pook *et al.*, 2019).

195 ***ToMAGIC phenotyping***

196 A proof-of-concept for testing the potential of the MAGIC population for GWAS
197 analysis and detection of genomic regions associated with different types of traits was
198 performed by phenotyping the eight parents and the 354 ToMAGIC lines for a set of traits
199 from different plant organs. The traits evaluated included two related to fruit size (fruit
200 locule number and fruit weight), one to plant pigmentation (plant anthocyanin), two to
201 leaf morphology (lobing/serration and leaf complexity), and one to earliness (number of
202 leaves below the first inflorescence). Tomato fruits evaluated for fruit weight and cut
203 transversally for locule number counting. Presence of plant anthocyanin was observed in
204 vegetative plant parts (stem, branches, leaf veins or leaf area) and scored in a range from
205 0 (slight presence, mainly on the stem) to 4 (strong presence in all plant parts). Leaf
206 lobing/serration was scored in a range from 1 (lack of lobing/serration) to 7 (very serrated
207 leaf). Leaf complexity was screened using a binary classification for pinnate (0) and
208 bipinnate (1) compound leaves. The number of leaves below the first inflorescence was
209 recorded by counting the leaves of the primary shoot when the first flower bud was
210 visible. Pearson pair-wise coefficient of correlation (r) among traits was calculated, and
211 their significance was assessed using a Bonferroni correction at the p<0.05 probability
212 level (Hochberg, 1988) using R packages psych (Revelle, 2007) and corrplot (Wei and
213 Simko, 2017).

214 ***Genome-Wide Association Study (GWAS)***

215 Using the genotypic and phenotypic data collected from the ToMAGIC lines, GWAS
216 analyses were performed for the selected traits using the GAPIT software (v.3, Wang and
217 Zhang, 2021). General linear model (GLM), mixed linear model (MLM), and BLINK
218 analyses were conducted for the association study (Price *et al.*, 2006; Yu *et al.*, 2006;

219 Huang *et al.*, 2019). Comparison of models was displayed in roundness Manhattan plots
220 and QQ plots. The multiple testing was corrected with the Bonferroni and the false
221 discovery rate (FDR) methods (Holm, 1979; Benjamini and Hochberg, 1995) with a
222 significance level of 0.05 (Thissen *et al.*, 2002). SNPs with a limit of detection (LOD)
223 score (calculated as $-\log_{10}[\text{p-value}]$) exceeding these specified thresholds or cutoff values
224 in the three GWAS models were considered significantly associated with the traits under
225 evaluation. Associations were considered significant if the same SNP exceeded the cut-
226 off thresholds in at least two of the implemented models, indicating robustness. The top
227 significant SNPs and their neighboring SNPs were used to calculate the correlation
228 coefficient (r^2). SNPs with default r^2 values greater than 0.5 were considered for haplotype
229 block estimation. The R package geneHapR was used for haplotype statistics (Zhang *et*
230 *al.*, 2023a). The genes underlying the haplotype blocks were retrieved from the Heinz
231 1706 SL4.0 tomato reference genome (Hosmani *et al.*, 2019). Genes were considered as
232 potential candidates in controlling the assessed traits according to SnpEff software v 4.2
233 prediction (Cingolani *et al.*, 2012) of the eight MAGIC founders (Gramazio *et al.*, 2019).
234 The Integrative Genomics Viewer (IGV) tool was used for the visual exploration of
235 founder genome sequences to validate SnpEff results (Robinson *et al.*, 2023). A
236 conservative domain analysis was performed using the NCBI conserved domain server
237 (<https://www.ncbi.nlm.nih.gov/Structure/cdd/wrpsb.cgi>) to assess the predicted variants
238 at the protein level. The BLASTp (e-value cut-off of $1e^{-10}$) alignment tool and
239 EnsemblPlants browser were used to compare the homology of protein sequences
240 encoded by genes belonging to the same gene family. Haplotype and phenotype boxplots
241 and density plots were generated with the R package ggplot2 (Wickham, 2016). To assess
242 the significance of differences among different haplotypes pairwise *t*-tests were
243 performed.

244

245 **Results**

246 ***MAGIC population construction***

247 In the first stage of MAGIC population development, SLC and SP accessions of
248 different origins (Figure 1A) were inter-crossed pairwise (Figure 1B). These materials are
249 native to different geographic regions of South and Central America, mainly from
250 Ecuador and Northern Peru, and provide a representation of the Andean variability lost
251 during the domestication process in Mesoamerica (Figure 1A). They were selected since
252 they are considered genetic diversity reservoirs barely exploited in tomato breeding
253 (Gramazio *et al.*, 2020a). They include a wide molecular variability and phenotypic
254 diversity in plant and inflorescence architecture, leaf, flower, and fruit traits, together with
255 resistance or tolerance - in some of the founders - to biotic and abiotic stresses (Blanca *et*
256 *al.*, 2015), including water and salt stress adaptation (Martínez-Cuenca *et al.*, 2020). The
257 eight founders have previously been characterized morphoagronomically and their
258 genomes have been resequenced (Blanca *et al.*, 2015; Gramazio *et al.*, 2020a).

259 These weedy (SLC) and wild (SP) tomato species are cross-compatible (Gramazio *et*
260 *al.*, 2020a), and thus the manual inter-cross was successfully performed. As a result of
261 the inter-cross of the eight founders, the F₁ hybrids, and the DHY hybrids, 112 IC1
262 individuals were obtained. The subsequent inter-crossing following a chain pollination

263 scheme resulted in the obtention of 232 IC2 and 481 IC3 individuals. The latter
264 individuals were self-pollinated to produce 475 S1, 452 S2, 427 S3, 400 S4, and the final
265 population of 354 S5 (ToMAGIC) lines (Figure 1B).

266 **Genotyping**

267 A total of 4,268,587 SNPs were generated from the genotyping of the 354
268 ToMAGIC lines using a newly developed 12k probes tomato SPET panel (Aprea *et al.*,
269 in preparation). After filtering, 6,488 markers were retained for the subsequent GWAS
270 analysis. A higher marker density was observed in gene-rich regions located in distal
271 chromosomal regions (Figure 1C). The distribution of SNPs among the different tomato
272 chromosomes was fairly uniform, with an average marker density of 8.51 per Mb (Table
273 1). There was a marker average interval of 0.13 Mb with the broader marker intervals
274 being around the pericentromeric regions. The filtered markers cover 16.91% of the total
275 annotated genes. The residual heterozygosity of the ToMAGIC lines was on average
276 6.31%.

277

278 **Table 1.** Chromosome-wide distribution of the SNP positions used for the genome-wide
279 association study (GWAS) in the tomato MAGIC population.

| Chromosome | Markers | % Markers | Chromosome length (Mb) | Marker density (markers/Mb) | Marker interval (Mb) | | Genes | Covered genes |
|------------|---------|-----------|------------------------|-----------------------------|----------------------|---------|--------|---------------|
| | | | | | Max. | Average | | |
| 1 | 646 | 10.78 | 90.86 | 7.11 | 3.60 | 0.14 | 4,133 | 619 |
| 2 | 568 | 7.25 | 53.47 | 10.62 | 3.77 | 0.09 | 3,379 | 518 |
| 3 | 624 | 8.30 | 65.30 | 9.56 | 2.52 | 0.10 | 3,324 | 578 |
| 4 | 815 | 8.75 | 64.46 | 12.64 | 1.32 | 0.08 | 2,819 | 689 |
| 5 | 656 | 8.44 | 65.27 | 10.05 | 1.57 | 0.10 | 2,382 | 496 |
| 6 | 408 | 7.84 | 47.26 | 8.63 | 3.11 | 0.11 | 2,769 | 392 |
| 7 | 425 | 8.07 | 67.88 | 6.26 | 2.97 | 0.16 | 2,517 | 379 |
| 8 | 346 | 8.14 | 64.00 | 5.41 | 3.35 | 0.19 | 2,428 | 315 |
| 9 | 436 | 8.02 | 68.51 | 6.36 | 4.26 | 0.16 | 2,521 | 403 |
| 10 | 406 | 7.46 | 64.79 | 6.27 | 2.58 | 0.16 | 2,52 | 342 |
| 11 | 552 | 7.51 | 54.38 | 10.15 | 1.69 | 0.10 | 2,326 | 446 |
| 12 | 606 | 9.43 | 66.69 | 9.09 | 1.97 | 0.11 | 2,444 | 498 |
| Total | 6,488 | 100 | 772.87 | | | | 33,562 | 5,675 |
| Average | | 8.33 | | 8.51 | | 0.13 | | |

280

281

282 **Population structure**

283 A lack of genetic structure in ToMAGIC population was supported by the Principal
284 Component Analysis (PCA), in which no differentiated groups were observed (Figure
285 2A). The first two PCs accounted only for 3.40% of the genetic variance, the first ten PCs
286 9.93%, and it required 41 PCs to explain 20% of the genetic variation, underscoring the
287 weak population structure of the population. In addition, kinship coefficients between
288 pairs of ToMAGIC lines varied from 0 to 1.32 (on a scale of 0 to 2), with 98.35% of the
289 pairs with kinship values <0.5 (Figure 2B). These results revealed a low genetic
290 relatedness among ToMAGIC lines.

291 SLC founders were grouped close together, with negative values of the PC1, while
292 SP founders had positive values for the PC1 (Figure 2A). A similar grouping was
293 observed in the dendrogram of the MAGIC population and founders (Figure 2C). SLC2
294 and SLC3 are the closest accessions to cultivated tomato and plot in the first PCA
295 quadrant with low values for the PC1 and high for the PC2. SLC4 is the closest to SP
296 founders in the PCA (Figure 2A) and is separated from the rest of SLC founders in the
297 dendrogram (Figure 2C). The estimated average contribution of each founder to the
298 overall population was around the theoretically expected value of 12.50%, with the range
299 varying from 11.62% for SP2 to 14.16% for SP4. However, the reconstruction of genome
300 mosaics for the 354 ToMAGIC lines, considering the eight founder haplotypes, revealed
301 different haplotype block proportions at different chromosomal positions (Figure 2D).

302 **Phenotyping analysis**

303 Phenotyping for locule number, fruit weight, plant anthocyanin pigmentation, leaf
304 lobing/serration, leaf complexity, and number of leaves below the first inflorescence
305 revealed a wide range of variation, including transgressive lines for some of the studied
306 traits (Table 2, Figure S1A). For the locule number trait, the average for SP founders was
307 2 lobules, while the average for SLC was 2.75 and the range between 2 and 4. However,
308 ToMAGIC lines with up to 5 and 6 locules were identified, although most of the lines
309 only had 2 locules, resulting in an average value of 2.2. For the fruit weight, ToMAGIC
310 lines showed an intermediate average (2.72 g) between the SP and SLC founders weight
311 averages of 1.60 g and 4.97 g, respectively. However, the range of variation of the
312 founders was greater (from 0.97 g to 11.59 g) than those of the ToMAGIC lines (0.44 to
313 7.01), and no lines were found with a higher weight than the heaviest founder (SLC3).
314 For the plant anthocyanin pigmentation, the mean of SLC founders (0.50) was lower than
315 that of the SP founders (1.25), mainly due to the high level of plant pigmentation of the
316 SP4 founder. The range of variation was greater for the ToMAGIC lines (from 0 to 4)
317 than for the founders (from 0 to 3). For the leaf lobing/serration, ToMAGIC lines showed
318 an intermediate average (3.69 g) between the SP and SLC founders averages of 2.50 and
319 6, respectively. The ToMAGIC lines covered all the variation range found in the founders,
320 from the lack of lobing/serration (1) to very serrated leaves (7). For the leaf complexity,
321 ToMAGIC lines showed an intermediate average (0.26) between the SP (0) and SLC
322 (0.50) founders. For the number of leaves below the first inflorescence, the SP founders
323 had a slightly lower number (4.33) than SLC founders (6.66), while ToMAGIC lines had
324 an average of 5.36 leaves. However, the range of variation was much larger for the
325 ToMAGIC lines (from 4 to 10) than for the founders (from 4 to 7). Pearson pairwise
326 correlations among the traits evaluation were conducted, and only a slight positive
327 correlation ($r = 0.3261$; $p=1.57e^{-7}$) between leaf lobing/serration and leaf complexity, was
328 observed (Figure S1B).

329

330 **Table 2.** Means and range values for SLC and SP founders and ToMAGIC lines for the
331 phenotypic traits evaluated.

332

| Trait | SLC | | SP | | ToMAGIC lines | |
|------------------------------------------------|---------|--------------|---------|-------------|---------------|-------------|
| | Average | Range | Average | Range | Average | Range |
| Locule number | 2.75 | 2 - 4 | 2 | 2 | 2.20 | 2 - 6 |
| Fruit weight | 4.97 | 1.61 - 11.59 | 1.60 | 0.97 - 2.89 | 2.72 | 0.44 - 7.01 |
| Plant anthocyanin | 0.50 | 0 - 1 | 1.25 | 0 - 3 | 0.94 | 0 - 4 |
| Leaf lobing and serration | 6 | 5 - 7 | 2.50 | 1 - 3 | 3.69 | 1 - 7 |
| Leaf complexity | 0.50 | 0 - 1 | 0 | 0 | 0.26 | 0 - 1 |
| Number of leaves below the first inflorescence | 6.66 | 6 - 7 | 4.33 | 4 - 5 | 5.36 | 4 - 10 |

333

334

335 **Fruit size**

336 *Locule number*

337 The Manhattan plot for fruit locule number revealed one significant peak on
 338 chromosome 2 (Figure 3A, Table 3). For the GLM model, 25 SNPs were above the FDR
 339 threshold (LOD > 4.15), 20 of them over the Bonferroni threshold (LOD > 5.11) between
 340 44.78 and 46.13 Mb. For the MLM model, 15 SNPs were above the FDR threshold, nine
 341 of them over the Bonferroni threshold between a reduced region of 44.82 and 46.02 Mb
 342 (Figure 3B). For the BLINK model, a single SNP was above the FDR and Bonferroni
 343 thresholds (LOD = 15.27) at 45.87 Mb position. This association peak accounted for
 344 26.84% of the total phenotypic variance of the locule number trait.

345

346 **Table 3.** Association analysis results for GLM, MLM, and BLINK models and list of
 347 candidate genes for locule number, fruit weight, plant anthocyanin, leaf lobing/serration,
 348 leaf complexity, and number of leaves below the first inflorescence.

| Trait | GLM | | | MLM | | | BLINK | | | Candidate genes | | |
|------------------------------------------------|------------|---------------------|-------|------------|---------------------|-------|------------|---------------------|-------|------------------|--------------------|-------------------------|
| | Chromosome | Genomic region (Mb) | LOD | Chromosome | Genomic region (Mb) | LOD | Chromosome | Genomic region (Mb) | LOD | Abbreviation | Name | Position (bp) |
| Locule number | 2 | 44.78 - 46.13 | 11.34 | 2 | 44.82 - 46.02 | 9.92 | 2 | 45.87 | 15.27 | <i>WUSCHEL</i> | Solyc02g083950.3.1 | 45,191,157 - 45,192,582 |
| Fruit weight | 2 | 50.51 - 50.55 | 5.21 | - | - | - | 2 | 50.55 | 5.33 | <i>FW2.2</i> | Solyc02g090730.3.1 | 50,292,691 - 50,293,481 |
| Plant anthocyanin | 7 | 8.38 - 61.70 | 15.28 | 7 | 59.97 - 60.88 | 12.42 | 7 | 60.44 | 21.14 | <i>SIMTB-ATV</i> | Solyc07g052490.4.1 | 60,912,702 - 60,913,855 |
| | 2 | 27.13 - 33.38 | 5.14 | - | - | - | 2 | 33.38 - 46.91 | 7.64 | <i>bHLH</i> | Solyc02g063430.4.1 | 33,546,773 - 33,549,186 |
| Leaf lobing and serration | 4 | 62.30 - 63.23 | 11.63 | 4 | 62.30 - 62.91 | 9.84 | 4 | 62.87 | 6.46 | <i>AP3/DEF</i> | Solyc04g081000.3.1 | 63,032,681 - 63,036,255 |
| | | | | | | | | | | <i>OMATE9</i> | Solyc04g080210.1.1 | 62,437,899 - 62,438,699 |
| | | | | | | | | | | <i>ANT</i> | Solyc04g077490.3.1 | 60,418,478 - 60,421,941 |
| Leaf complexity | 4 | 62.49 - 62.73 | 5.84 | 4 | 62.49 | 5.38 | 4 | 62.49 | 8.93 | <i>KNOTTED1</i> | Solyc04g077210.3.1 | 60,124,304 - 60,131,770 |
| | | | | | | | | | | <i>IA49</i> | Solyc04g076850.3.1 | 59,750,087 - 59,755,552 |
| | | | | | | | | | | <i>FT1</i> | Solyc11g008640.1.1 | 2,854,837 - 2,857,237 |
| | | | | | | | | | | <i>FT2</i> | Solyc11g008650.1.1 | 2,866,945 - 2,867,166 |
| Number of leaves below the first inflorescence | 11 | 2.05 - 2.80 | 9.19 | 11 | 2.17 - 2.80 | 8.54 | 11 | 2.80 | 24.22 | <i>SP1</i> | Solyc11g007880.1.1 | 2,135,303 - 2,135,602 |
| | | | | | | | | | | <i>J</i> | Solyc11g010570.2.1 | 3,671,232 - 3,676,350 |

349

350

351 In the genomic candidate region on chromosome 2, the *WUSCHEL* gene
 352 (Solyc02g083950.3.1, 45,191,157-45,192,582 bp) was identified (Table 3). *WUSCHEL*
 353 gene controls stem cell fate in the apical meristem directly affecting locule number during
 354 tomato fruit development (Barrero *et al.*, 2006; Muños *et al.*, 2011). The two multi-locular
 355 founders of the ToMAGIC population, SLC2 and SLC3, showed two SNPs immediately
 356 downstream of the *WUSCHEL* gene that were previously described as directly associated
 357 with an increased locule number (Muños *et al.*, 2011). Specifically, a T/C transition at
 358 45,189,386 bp and a A/G transition at 45,189,392 bp are considered as the responsible
 359 SNPs for the locule number trait (Figure S1A). These two SNPs were in almost complete
 360 linkage disequilibrium, and they are considered as a unique haplotype.

361 Haplotype analyses were performed to associate the candidate genomic regions with
362 the phenotypic effects. For the locule number, a significant difference was observed
363 between the haplotype of the SLC2 and SLC3 founders, which are the ones showing more
364 than 2 locules, and the rest of the haplotypes of the ToMAGIC founders according to
365 pairwise *t*-test for multiple comparisons (Figure 4A). When generating the density plot,
366 higher values were also associated with the SLC2 (at 3 locules) and SLC3 (at 4 locules)
367 founder haplotype.

368 *Fruit weight*

369 The Manhattan plot for fruit weight also revealed one significant peak on
370 chromosome 2, although only for GLM and BLINK models (Figure S2A, Table 3). For
371 the GLM model, three peaks were above the Bonferroni threshold ($LOD > 5.11$) between
372 50.51 and 50.55 Mb (Figure S2B). For the BLINK model, a single SNP was above the
373 Bonferroni threshold ($LOD = 5.33$) at 50.55 Mb position. This association peak explained
374 14.76% of the total phenotypic variance of the fruit weight trait.

375 Under the significant peak on chromosome 2, the well-known *FW2.2* gene
376 (Solyc02g090730.3.1, 50,292,691-50,293,481 bp) was identified (Table 3). This gene is
377 differentially expressed in floral development and controls carpel cell division (Frary *et*
378 *al.*, 2000). The wild-type SNP was identified in all the ToMAGIC founders, except for
379 founders SLC2 and SLC3, which have larger fruit weights (Blanca *et al.*, 2015). This SNP
380 corresponds to a C/T change upstream of the 5' region of *FW2.2* gene at 50,292,019 bp
381 (Figure S1A).

382 In the haplotype analysis, pairwise *t*-test revealed a significant difference between
383 SLC2 and SLC3 on one side and SP founders from the other (Figure 4B). When
384 generating the density plot, most of the lines are around 2 to 3 g since light fruits
385 predominate in the ToMAGIC population with an average weight of 2.72 g (Table 2).
386 Lines with weights greater than 3 show mostly SLC2 and SLC3 haplotypes.

387 *Plant pigmentation*

388 The Manhattan plot for plant anthocyanin revealed two significant peaks: one major
389 peak on chromosome 7 and one minor but significant peak on chromosome 2 (Figure
390 S3A, Table 3). For the GLM model, 31 SNPs were above the FDR threshold ($LOD >$
391 3.80) on chromosome 7, 21 of them over the Bonferroni threshold ($LOD > 5.11$) between
392 8.38 and 61.70 Mb. On chromosome 2, only four SNPs were above the FDR threshold,
393 being two of them over the Bonferroni threshold between 27.13 and 33.38 Mb. For the
394 MLM model, only one association peak was identified on chromosome 7 with eight SNPs
395 over the FDR threshold, five of them over the Bonferroni threshold between a reduced
396 region of 59.97 and 60.88 Mb (Figure S3B). For the BLINK model, a single SNP was
397 above the FDR and Bonferroni thresholds ($LOD = 21.14$) on chromosome 7 at 60.44 Mb
398 position. On chromosome 2, only two SNPs were above the FDR and Bonferroni
399 thresholds at 33.38 and 46.91 Mb positions ($LOD = 7.64$ and 6.70 , respectively). The
400 association peak on chromosome 7 explained 15.14% of the total phenotypic variance of
401 the plant anthocyanin trait, while the peak on chromosome 2 explained 4.68% of the
402 phenotypic variance.

403 Under the major GWAS peak on chromosome 7, in the genomic region of
404 60,912,702-60,913,855 bp, a *MYB-like* transcription factor (*SlMYB-ATV*,
405 Solyc07g052490.4.1) was identified (Table 3). The *SlMYB-ATV* (myeloblastosis-
406 atroviolacea) gene has been described as a repressor of anthocyanin synthesis in
407 vegetative tissues of tomato plants (Colanero *et al.*, 2018). However, we did not observe
408 the previously described mutations in the gene sequence in our accessions. In contrast, a
409 9-bp in frame deletion at 60,912,903 bp position, deleting 3 amino acids in the
410 transcriptional repressor MYB domain was identified in the SP4 founder, which is the
411 unique founder showing anthocyanins in all plant parts (Figure S1A).

412 The same procedure was followed for the minor peak on chromosome 2. All the
413 genes located near or within the LD block were assessed by SnpEff (Cingolani *et al.*,
414 2012) for all of the MAGIC founders. However, no potential candidate genes were
415 identified, since no high-effect variants were predicted distinguishing between
416 anthocyanin-containing and anthocyaninless founders.

417 In the haplotype analysis for chromosome 7, a significant difference was observed
418 between the SP4 founder, which is the one showing increased levels of plant
419 anthocyanins, and the rest of ToMAGIC founders according to pairwise *t*-test (Figure
420 4C). When generating the density plot, higher anthocyanin values were also associated
421 with the SP4 founder haplotype.

422 *Leaf morphology*

423 *Leaf lobing/serration*

424 The Manhattan plot for leaf lobing/serration revealed one significant peak on
425 chromosome 4 (Figure S4A, Table 3). For the GLM model, 13 SNPs were above the FDR
426 threshold (LOD > 4.81), ten of them over the Bonferroni threshold (LOD > 5.11) between
427 62.30 and 63.23 Mb. For the MLM model, ten SNPs were above the FDR threshold, nine
428 of them over the Bonferroni threshold between a reduced region of 62.30 and 62.91 Mb
429 (Figure S4B). For the BLINK model, a single SNP was above the FDR and Bonferroni
430 thresholds (LOD = 6.46) at 62.87 Mb position. This association peak accounted for
431 53.84% of the total phenotypic variance of the leaf lobing/serration trait.

432 Different genes involved in the leaf shape were detected within the candidate
433 genomic region on chromosome 4 identified in the GWAS for the leaf lobing/serration
434 (Table 3). In order of proximity to the candidate region, we found the
435 *APETALA3/DEFICIENS* or *AP3/DEF* gene (Solyc04g081000.3.1 between 63,032,681-
436 63,036,255 bp), which has been described as a regulator of petal and sepal development
437 (Quinet *et al.*, 2014), the ovate family protein 9 or *OVATE9* gene (Solyc04g080210.1.1
438 between 62,437,899-62,438,699 bp) which belongs to a family protein that regulates
439 different plant organs shape, including cotyledons, leaves, and fruits (Snouffer *et al.*,
440 2020), and the *AP2-like* ethylene-responsive transcription factor *AINTEGUMENTA* or
441 *ANT* gene (Solyc04g077490.3.1 between 60,418,478-60,421,941 bp), which plays a role
442 as an auxin regulator in shoot and flower meristem maintenance, organ size and polarity,
443 flower initiation, ovule development, floral organ identity, cell proliferation (Horstman
444 *et al.*, 2014). No high-effect variants were predicted by SnpEff in the coding sequence of
445 these genes contrasting for the different founders' phenotypes.

446 Haplotype results revealed a significant difference between SLC and SP founders
447 according to pairwise *t*-test (Figure 4D). Although the haplotypes density plot also did
448 not show a bimodal distribution for SLC and SP founders, it showed a higher density for
449 SP haplotypes in lines exhibiting lack of lobing/serration or moderate lobing values, and
450 a slightly higher density for SLC haplotypes in the very serrated leaf values.

451 *Leaf complexity*

452 The Manhattan plot for leaf complexity revealed one significant peak on
453 chromosome 4 (Figure S5A, Table 3). For the GLM model, two SNPs were above the
454 Bonferroni threshold (LOD > 5.11) between 62.49 and 62.73 Mb (Figure S5B). For the
455 MLM and BLINK model, a single SNP was above the Bonferroni threshold (LOD = 5.38
456 and 8.93, respectively) at 62.49 Mb position. This association peak accounted for 4.12%
457 of the total phenotypic variance of the leaf complexity trait.

458 Two genes involved in the leaf complexity were detected within the candidate
459 genomic region on chromosome 4 identified in the GWAS (Table 3). In order of
460 proximity to the candidate region we found the *KNOTTED1* gene (Solyc04g077210.3.1
461 between 60,124,504-60,131,770 bp) which is expressed during leaf development and
462 affects leaf morphology altering leaf complexity (Shani *et al.*, 2009), and the *entire* or
463 *INDOLE-3-ACETIC ACID9 IAA9* gene (Solyc04g076850.3.1 between 59,750,087-
464 59,755,552 bp), which controls leaf morphology from compound to simple leaves (Zhang
465 *et al.*, 2007). No high-effect variants were predicted by SnpEff in the coding sequence of
466 these genes for the founders with contrasting phenotypes.

467 Haplotype results revealed a significant difference between SLC and SP founders
468 according to the pairwise *t*-test (Figure 4E). Although the haplotypes density plot did not
469 show a bimodal distribution for SLC and SP founders, it showed a higher density for SP
470 haplotypes in pinnate leaves, and a slightly higher density for SLC haplotypes in the
471 bipinnate leaves.

472 *Earliness*

473 The Manhattan plot for the number of leaves below the first inflorescence revealed
474 one significant peak on chromosome 11 (Figure S6A, Table 3). For the GLM model, four
475 SNPs were above the FDR and Bonferroni thresholds (LOD > 4.75 and 5.11, respectively)
476 between 2.05 and 2.80 Mb. For the MLM model, only two SNPs were above the FDR
477 and Bonferroni thresholds between a reduced region of 2.17 and 2.80 Mb (Figure S6B).
478 For the BLINK model, a single SNP was above the FDR and Bonferroni thresholds (LOD
479 = 24.22) at 2.80 Mb position. The association peak explained 5.52% of the total
480 phenotypic variance of the number of leaves below the first inflorescence trait.

481 Different genes implicated in the flowering pathway were identified in the candidate
482 genomic region on chromosome 11 proposed in the GWAS for the number of leaves
483 below the first inflorescence (Table 3). In order of proximity to the candidate region we
484 found two *FLOWERING LOCUS T (FT)* genes (*FT1* Solyc11g008640.1.1 between
485 2,854,837- 2,857,237 bp and *FT2* Solyc11g008650.1.1 between 2,866,945-2,867,166
486 bp), which have been described as mediating the onset of flowering and the floral
487 transition in all angiosperms (Pin and Nilsson, 2012), the *SELF-PRUNING*
488 *INTERACTING PROTEIN 1* or *SP1* gene (Solyc11g007880.1.1 between 2,135,303-

489 2,135,602 bp), which is involved in a conserved signalling system that regulates
490 flowering (Pnueli *et al.*, 2001), and the *JOINTLESS* or *J* gene (Solyc11g010570.2.1
491 between 3,671,232-3,676,350 bp), which plays a role in flowering promotion
492 (Szymkowiak and Irish, 2006). The FT1 and FT2 proteins have respectively a 71.68%
493 (124/173) and 87.69% (57/65) identity with the well-known *SINGLE-FLOWER TRUSS*
494 (*SFT*, Solyc03g063100.2.1) gene product according to BLASTp alignment. While *FT1* is
495 recognized as a parologue of the *SFT* gene in EnsemblPlants, *FT2* seems to be a truncated
496 pseudogene. Nevertheless, no clear variants were predicted by SnpEff in the coding
497 sequence of these genes contrasting for the different founders' phenotypes.

498 Haplotype results did not differentiate between SLC and SP founders (Figure 4F).
499 Pairwise *t*-test only revealed a significant difference between SLC1, SLC3, and SLC4
500 from SLC2, SP1, and SP2 founders, with SP3 and SP4 in intermediate positions. The
501 haplotype density plot also did not show a bimodal distribution for SLC and SP founders.
502 However, it showed a trend for lower number leaves below the first inflorescences for the
503 SP haplotypes, while SLC haplotypes were distributed along a wide range of number of
504 leaves below the first inflorescence.

505

506 Discussion

507 We present a novel inter-specific ToMAGIC population of 354 lines constructed by
508 combining the genomes of SLC and SP founders. SLC accessions are phylogenetically
509 positioned between SP and cultivated tomato (Blanca *et al.*, 2015, 2022). Therefore,
510 founders were selected to exploit the wide diversity found in the tomato closest relatives
511 taking advantage of their interbreeding compatibility (Peralta *et al.*, 2008). Previous
512 resequencing of the selected founders allowed to significantly enhance recombination
513 detection, haplotype prediction, and causal variants identification within the MAGIC
514 population (Gramazio *et al.*, 2020a).

515 The MAGIC population was generated through a systematic “funnel” approach
516 (Arrones *et al.*, 2020) involving multiple rounds of inter-cross of the eight selected
517 founders and five generations of selfing, totalling ten generations. The three inter-
518 crossing generations from the two double hybrids and the blind SSD process ensured high
519 levels of recombination, maintaining a high genetic and morphological diversity. The
520 ToMAGIC lines were genotyped by using a newly developed 12k probes tomato panel,
521 based on SPET, which is a robust technology based on target SNPs, but also capable of
522 discovering novel SNPs (Barchi *et al.*, 2019). Although SPET has been mostly used in
523 the biomedical field, it has demonstrated its potential as a high-throughput and high-
524 efficiency genotyping platform in *Solanum* species (Gramazio *et al.*, 2020b; Mangino *et*
525 *al.*, 2022). In this study, more than 4 million SNPs were generated with the 12k probes
526 tomato SPET panel. After stringent filtering, 6,488 were retained as markers, while in the
527 previous tomato MAGIC population developed by Pascual *et al.* (2015), 1,486 markers
528 obtained by a custom-made genotyping platform (Fluidigm 96.96 Dynamic Arrays, San
529 Francisco, CA) were used for population analyses. The genotypic data revealed the
530 absence of genetic structure, which is one of the advantages of MAGIC populations
531 (Arrones *et al.*, 2020), and a balanced representation of the founder genomes. The average

532 contribution of each founder to the overall population was around 12.50%, which is the
533 expected value for a population developed from eight founders.

534 We have demonstrated the power of our ToMAGIC population for the fine mapping
535 of traits of interest in tomato breeding. Specifically, GWAS analysis detected strong
536 associations for all the traits evaluated using three different models (GLM, MLM, and
537 BLINK), supporting the robustness of the associations detected (Price *et al.*, 2006; Yu *et*
538 *al.*, 2006; Huang *et al.*, 2019).

539 The implementation of SLC and SP accessions as founders have introduced a wide
540 genetic and phenotypic diversity in the ToMAGIC population (Blanca *et al.*, 2015;
541 Gramazio *et al.*, 2020a). Our proof-of-concept, focusing on a subset of traits from
542 different plant parts has revealed a large phenotypic diversity in the ToMAGIC
543 population, including transgressive lines to some of the founders for all traits except leaf
544 morphology. Within the phenotypic diversity of the final population, wild alleles showed
545 a dominant effect over domesticated alleles in most traits. For instance, ToMAGIC lines
546 tend to produce small fruits and simpler leaves, more similar to SP than to cultivated
547 tomato. This prevalent dominance of wild alleles has been previously observed during
548 the development of other inter-specific populations (Semel *et al.*, 2006).

549 Large tomato fruit size is a typical domestication trait, controlled by at least five
550 different genes (Pereira *et al.*, 2021). It is tempting to speculate that, similar to the non-
551 shattering spike trait in cereals (Lin *et al.*, 2012), it negatively affects plant fitness in the
552 wild, by reducing seed dispersal by small vertebrates. Drawing on this parallel, the most
553 likely scenario is that recessive alleles for large fruit size in tomato and non-shattering
554 spike in cereals were both pre-existing in wild/weedy populations, and that they were not
555 completely counterselected due to their recessive nature. Under this scenario, human
556 selection for higher harvestable biomass probably acted on the rare homozygous plants
557 that appeared in these wild populations. Consistent with this hypothesis, the
558 nonfunctional (domesticated) allele of the rice shattering gene *sh4* is found, at low
559 frequency, in the wild ancestor *O. rufipogon* (Lin *et al.*, 2007).

560 Almost all wild tomato species produce bilocular small fruits, and therefore, locule
561 number and fruit weight played a crucial role in the increase in fruit size during
562 domestication (Alpert *et al.*, 1995; Lippman and Tanksley, 2001; Barrero *et al.*, 2006).
563 On one hand, as a result of the GWAS analysis for locule number, an associated genomic
564 region was identified that colocalized with the *WUSCHEL* gene. Mutations on this gene
565 have been necessary to increase locule number during domestication (Muños *et al.*, 2011).
566 However, previous sequence analysis on this gene revealed that the diversity of this locus
567 was drastically reduced in the cultivated species (Muños *et al.*, 2011; van der Knaap *et*
568 *al.*, 2014). Only two SNPs have been identified in this gene responsible for the large-
569 fruited phenotype, which are the same two SNPs that we have found in our population.
570 On the other hand, the GWAS analysis for fruit weight revealed an associated genomic
571 region on chromosome 2 between 50.51 and 50.55 Mb in the region where the *FW2.2*
572 gene is located (Frary *et al.*, 2000). Similarly, but not as precisely as in our ToMAGIC
573 populations, in the tomato MAGIC developed by Pascual *et al.* (2015) a peak with the
574 highest LOD value between 46.35 and 47.49 Mb was also identified. The *FW2.2* gene is
575 responsible for up to 30% of the fruit weight variation between large domesticated

576 tomatoes and the small-fruited wild relatives (Nesbitt and Tanksley, 2001). All modern
577 tomatoes contain the large-fruited allele for *FW2.2* (Blanca *et al.*, 2015; Beauchet *et al.*,
578 2021), which was also identified in the two large-fruited SLC ToMAGIC founders.
579 Molecular evolutionary studies suggested that this allele originated in wild tomatoes long
580 before the process of domestication (Nesbitt and Tanksley, 2002). Indeed, fruit weight
581 was strongly selected in SLC in the Andean region of Ecuador and Northern Peru prior
582 to the domestication of tomato in Mesoamerica (Blanca *et al.*, 2015).

583 Anthocyanins are the main responsible for purple pigmentation in tomato leaf veins,
584 leaf tissues, and stem (Barrett *et al.*, 2010; Jaakola, 2013). Plant anthocyanins are more
585 commonly present in wild tomato species, where they have a main protective function
586 against UV-visible light and other stressful conditions such as cold temperature,
587 pathogens, or drought (Gould, 2004; Olsen *et al.*, 2009; Zhang *et al.*, 2014). The GWAS
588 results identified an associated genomic region which colocalized with the previously
589 described *SlMYB-ATV* gene. Overexpression of the coding protein acts as an inhibitor of
590 anthocyanin production by silencing key regulators of the biosynthesis pathway (Cao *et*
591 *al.*, 2017; Colanero *et al.*, 2018). The *atv* mutation was described as a 4 bp insertion in
592 the second exon which led to a frameshift variant resulting in a premature stop codon with
593 a strong impact in the polypeptide. This mutation was identified as the causal agent of
594 anthocyanin production in the vegetative part of the plant (Colanero *et al.*, 2018). Here, a
595 novel mutation in the “purple” SP4 founder was found. Specifically, a 9 bp deletion
596 leading to a disruptive inframe deletion which directly affects the transcription repressor
597 MYB domain was identified. This demonstrates the significance of the ToMAGIC
598 population as a reservoir of novel candidate genes and causative alleles. Interestingly, of
599 the four SP founders, SP4 is the only one showing anthocyanin pigmentation as well as
600 the one collected at the highest altitude (1,020 m) and lowest mean annual temperature
601 (13°C), in agreement with the proposed role of anthocyanins as UV-screens in cold
602 temperatures (Martínez-Cuenca *et al.*, 2020).

603 Cultivated tomato leaf morphology has typical bipinnate compound leaves with
604 moderately deep lobes, while there is a huge diversity of leaf morphology among wild
605 tomato species (Zhang *et al.*, 2007; Kang *et al.*, 2010; Nakayuma *et al.*, 2023). Since leaf
606 lobing/serration and leaf complexity traits are correlated, both traits have usually been
607 studied together (Kang *et al.*, 2010). Actually, the GWAS results identified an associated
608 genomic region on chromosome 4 around 62 Mb position for both traits, and candidate
609 genes affecting both traits were identified within this genomic region. Although the
610 *AP3/DEF* gene has mainly been related to petal and sepal development, other genes
611 belonging to the same MADS box family are involved in tomato leaf development.
612 Specifically, the *APETALA1/FRUITFULL (AP1/FUL)* MADS box genes are involved in
613 the organogenic activity of the leaf margin and leaf complexity (Burko *et al.*, 2013). The
614 *ANT* gene also belongs to a family of APETALA 2/ETHYLENE RESPONSE FACTOR
615 (AP2/ERF) domain transcription factors which affects plant leaf shape and size by
616 regulating cell proliferation (Horstman *et al.*, 2014). The *OVATE* gene was first identified
617 in tomato as a key regulator of fruit shape (Wang *et al.*, 2016). However, expression of
618 *OVATE* genes can also result in dwarf plants with shorter and thicker organs such as
619 rounder leaves (Snouffer *et al.*, 2020). The tomato *KNOTTED1* promotes cytokinin
620 biosynthesis which is directly related to cell proliferation (Nakayuma *et al.*, 2023), and
621 different levels of cytokinins led to a broad spectrum in leaf complexity (Shani *et al.*,

622 2009; Shwartz *et al.*, 2016). This gene has a key role in the molecular mechanism behind
623 leaf development and evolution and has been repeatedly exploited to generate natural
624 variations in leaf shape (Ichihashi and Tsukaya, 2015). The *IAA9* gene is a transcriptional
625 repressor in auxin signal transduction (Abe-Hara *et al.*, 2021). Tomato mutants for *IAA9*
626 also showed altered leaf morphology with the compound leaf changing to a single leaf
627 (Zhang *et al.*, 2007; Ueta *et al.*, 2017; Abe-Hara *et al.*, 2021). In this way, leaf
628 development is mainly influenced by cell proliferation and different hormones as a result
629 of the activity of a complex gene network (Nakayuma *et al.*, 2023). An accurate
630 phenotyping of the ToMAGIC population for these traits has allowed to narrow down a
631 genomic region that harbours a large number of genes related to leaf morphology. This
632 genomic region could be further narrowed down by studying the segregation of the cross
633 between two isolines to enable the identification of the responsible gene/s.

634 The existence of early-flowering alleles in wild species indicates the relevance of
635 exploiting the genetic variation present in tomato wild relatives (Jiménez-Gómez *et al.*,
636 2007). Although the mechanisms controlling the transition from vegetative to
637 reproductive growth are complex, several genes involved in flowering regulation are
638 known (Meir *et al.*, 2021; Zhang *et al.*, 2023b). The number of leaves below the first
639 inflorescence trait is a proxy for earliness in tomato (Honma *et al.*, 1963) and is easily
640 scored and commonly assessed to evaluate the earliness in tomato (Jiménez-Gómez *et al.*,
641 2007; Nakano *et al.*, 2016; Silva *et al.*, 2019). The GWAS analysis for the number of
642 leaves below the first inflorescence identified an association on chromosome 11, where
643 several genes related to flowering time were found (two *FT* genes, *SP1*, and *J*). The most
644 studied *FT* gene is the tomato ortholog *SINGLE-FLOWER TRUSS* (*SFT*) gene on
645 chromosome 3, which encodes for florigen and induces flowering in day-neutral (Turck
646 *et al.*, 2008; Meir *et al.*, 2021; Zhang *et al.*, 2023b). Here, we report the *FT1* gene on
647 chromosome 11, a parologue of the *SFT* gene which may also be involved in the flowering
648 regulation. The *SP1* gene is a member of the *CETS* family of regulatory genes, together
649 with *FT* genes, controlling flowering time (Pnueli *et al.*, 2001). However, they play an
650 antagonistic role, since *SP1* delays flowering in tomato (Zhang *et al.*, 2023b). The *J* gene
651 is involved in the same pathway as the *SFT* gene but with a small role in flowering
652 promotion (Szymkowiak and Irish, 2006; Zhang *et al.*, 2023b). A better understanding of
653 the mechanisms underlying the tomato flowering regulatory pathways will allow breeding
654 to target more precise candidate genes for the induction of early flowering. Nevertheless,
655 once again, the ToMAGIC population has led us to a genomic region directly involved in
656 the transition to flowering, pointing to new candidate genes.

657 Overall, the genotyping results together with the large morphological variation
658 observed in the new inter-specific SLC/SP tomato MAGIC population, as well as the
659 appearance of transgressive phenotypes, indicate that recombination and variation were
660 maximised in the final population. The ToMAGIC population has demonstrated a high
661 potential for the fine mapping of traits of interest from different plant parts. Given the fact
662 that the population contains representatives of the tomato ancestor (SP) and the primitive
663 weedy forms (SLC) of tomato, it can also be a tool of great relevance for studying the
664 genetic changes in the early stages of tomato domestication. It is also evident from our
665 study that the derived ToMAGIC population or core collections developed from it can
666 contribute to tomato genetics research and breeding programs. Recombinant lines with

667 combinations of traits of interest present in different founders can also be of direct interest
668 to breeders or even for selection of small-fruited new cultivars.

669

670 **Acknowledgements**

671 Funding for this work has been received from the following funders:
672 MCIN/AEI/10.13039/501100011033 (grant PID2020-118627RB-I00), MCIN/AEI
673 /10.13039/501100011033 and European Union Europea NextGenerationEU/ PRTR
674 (grant TED2021-129296B-I00), Conselleria d'Innovació, Universitats, Ciència i Societat
675 Digital of the Generalitat Valenciana (grant CIPROM/2021/020), European Commission
676 H2020 Research and Innovation Programme through the HARNESSSTOM innovation
677 action (grant agreement No. 101000716) and the Horizon Europe PRO-GRACE project
678 (grant agreement No. 10194738). Andrea Arrones is grateful to Spanish Ministerio de
679 Ciencia, Innovación y Universidades for a predoctoral (FPU18/01742) contract. Oussama
680 Antar is grateful to Conselleria d'Innovació, Ciència i Societat Digital of the Generalitat
681 Valenciana for a pre-doctoral grant within the Santiago Grisolía program
682 (CIGRIS/2022/113). Leandro Pereira-Dias is grateful to Universitat Politècnica de
683 Valencia and the Spanish Ministerio de Universidades for a post-doctoral grant under the
684 Margarita Salas funded by the European Union NextGenerationEU/PRTR. Pietro
685 Gramazio is grateful to Spanish Ministerio de Ciencia e Innovación for a post-doctoral
686 grant (RYC2021-031999-I) funded by MCIN/AEI/10.13039/501100011033 and the
687 European Union through NextGenerationEU/PRTR.

688

689 **Contributions**

690 SV, PG, MJD, and JP conceived the idea and supervised the manuscript; AA OA,
691 LP-D, AS, and MJD performed the field trials. GA and GG in collaboration with TECAN
692 Genomics designed the 12k SPET panel. All authors analysed the results. AA and OA
693 prepared a first draft of the manuscript and the rest of authors reviewed and edited the
694 manuscript. All authors have read and agreed to the published version of the manuscript.

695

696 **Data availability statement**

697 The datasets presented in this study can be found in online repositories. The names
698 of the repository/repositories and accession number(s) can be found below:
699 <https://www.ncbi.nlm.nih.gov/>, PRJNA616074.

700

701 **Conflict of interest**

702 The authors declare that the research was conducted in the absence of any
703 commercial or financial relationships that could be construed as a potential conflict of
704 interest.

705

706 **Supplementary information**

707 **Figure S1.** (A) A representation of different phenotypes for the locule number, fruit
708 weight, and plant anthocyanin traits, together with the known genes controlling these
709 traits indicating the phenotypic-causing variants. (B) Correlation analysis among all the
710 studied traits showing a slight positive correlation between the leaf morphology traits,
711 corresponding to leaf lobing/serration and leaf complexity. On the right, a representation
712 of the phenotypic scores for both traits.

713 **Figure S2.** Genome-wide association results for the fruit weight trait. (A) Manhattan plots
714 comparing GLM, MLM and BLINK models. (B) On the top, a chromosome-wise
715 Manhattan plot with the top significant markers. Bonferroni threshold is represented with
716 red dashed line. On the bottom, heat map of pairwise linkage disequilibrium (LD).

717 **Figure S3.** Genome-wide association results for the plant anthocyanin trait. (A)
718 Manhattan plots comparing GLM, MLM and BLINK models. (B) On the top, a
719 chromosome-wise Manhattan plot with the top significant markers. Bonferroni and FDR
720 thresholds are represented with red dashed and continuous lines, respectively. On the
721 bottom, heat map of pairwise linkage disequilibrium (LD).

722 **Figure S4.** Genome-wide association results for the leaf lobing/serration trait. (A)
723 Manhattan plots comparing GLM, MLM and BLINK models. (B) On the top, a
724 chromosome-wise Manhattan plot with the top significant markers. Bonferroni and FDR
725 thresholds are represented with red dashed and continuous lines, respectively. On the
726 bottom, heat map of pairwise linkage disequilibrium (LD).

727 **Figure S5.** Genome-wide association results for the leaf complexity trait. (A) Manhattan
728 plots comparing GLM, MLM and BLINK models. (B) On the top, a chromosome-wise
729 Manhattan plot with the top significant markers. Bonferroni threshold is represented with
730 red dashed line. On the bottom, heat map of pairwise linkage disequilibrium (LD).

731 **Figure S6.** Genome-wide association results for the number of leaves below the first
732 inflorescence trait. (A) Manhattan plots comparing GLM, MLM and BLINK models. (B)
733 On the top, a chromosome-wise Manhattan plot with the top significant markers.
734 Bonferroni and FDR thresholds are represented with red dashed and continuous lines,
735 respectively. On the bottom, heat map of pairwise linkage disequilibrium (LD).

736

737 **References**

738 Abe-Hara, C., Yamada, K., Wada, N., *et al.* (2021). Effects of the *sliaa9* mutation on
739 shoot elongation growth of tomato cultivars. *Front. Plant. Sci.*, *12*, 627832. doi:
740 10.3389/fpls.2021.627832

741 Alpert, K. B., Grandillo, S., and Tanksley, S. D. (1995). *fw* 2.2:a major QTL controlling
742 fruit weight is common to both red- and green-fruited tomato species. *Theor. Appl.*
743 *Genet.*, *91*, 994–1000. doi: 10.1007/BF00223911

744 Arrones, A., Vilanova, S., Plazas, M., Mangino, G., Pascual, L., Díez, M. J., *et al.* (2020).
745 The dawn of the age of multi-parent magic populations in plant breeding: Novel
746 powerful next-generation resources for genetic analysis and selection of
747 recombinant elite material. *Biology*, *9*, 229. doi: 10.3390/biology9080229

748 Barchi, L., Acquadro, A., Alonso, D., Aprea, G., Bassolino, L., Demurtas, O., *et al.*
749 (2019). Single Primer Enrichment Technology (SPET) for high-throughput
750 genotyping in tomato and eggplant germplasm. *Front. Plant Sci.*, *10*, 1005. doi:
751 10.3389/fpls.2019.01005

752 Barrero, L. S., Cong, B., Wu, F., and Tanksley, S. D. (2006). Developmental
753 characterization of the fasciated locus and mapping of *Arabidopsis* candidate genes
754 involved in the control of floral meristem size and carpel number in tomato. *Genome*,
755 *49*, 991–1006. doi: 10.1139/g06-059

756 Barrett, D. M., Beaulieu, J. C., and Shewfelt, R. (2010). Color, flavor, texture, and
757 nutritional quality of fresh-cut fruits and vegetables: desirable levels, instrumental
758 and sensory measurement, and the effects of processing. *Critical Reviews in Food
759 Sci. and Nutrition*, *50*, 369–389. doi: 10.1080/10408391003626322

760 Beauchet, A., Gévaudant, F., Gonzalez, N., and Chevalier, C. (2021). In search of the still
761 unknown function of *FW2.2/CELL NUMBER REGULATOR*, a major regulator of
762 fruit size in tomato. *J. Exp. Bot.*, *72*, 5300–5311. doi: 10.1093/jxb/erab207

763 Benjamini, Y., and Hochberg, Y. (1995). Controlling the false discovery rate: a practical
764 and powerful approach to multiple testing. *J. R. Stat. Soc.*, *57*, 289–300. doi:
765 10.1111/j.2517-6161.1995.tb02031.x

766 Blanca, J., Montero-Pau, J., Sauvage, C., Bauchet, G., Illa, E., Díez, M. J., *et al.* (2015).
767 Genomic variation in tomato, from wild ancestors to contemporary breeding
768 accessions. *BMC Genomics*, *16*, 257. doi: 10.1186/s12864-015-1444-1

769 Blanca, J., Sanchez-Matarredona, D., Ziarolo, P., Montero-Pau, J., Van der Knaap, E.,
770 Díez, M. J., *et al.* (2022). Haplotype analyses reveal novel insights into tomato
771 history and domestication driven by long-distance migrations and latitudinal
772 adaptations. *Horticulture Research*, *9*. doi: 10.1093/hr/uhac030

773 Bombarely, A., Menda, N., Tecle, I. Y., Buels, R. M., Strickler, S., Fischer-York, T., *et
774 al.* (2010). The sol genomics network (solgenomics.net): Growing tomatoes using
775 Perl. *Nucleic Acids Res.*, *39*, 1149–1155. doi: 10.1093/nar/gkq866

776 Bradbury, P. J., Zhang, Z., Kroon, D. E., Casstevens, T. M., Ramdoss, Y., and Buckler,
777 E. S. (2007). TASSEL: software for association mapping of complex traits in diverse
778 samples. *Bioinformatics*, *23*, 2633–2635. doi: 10.1093/bioinformatics/btm308

779 Burko, Y., Shleizer-Burko, S., Yanai, O., Shwartz, I., Zelnik, I. D., Jacob-Hirsch, J., *et
780 al.* (2013). A role for *APETALA1/FRUITFULL* transcription factors in tomato leaf
781 development. *Plant Cell*, *25*, 2070–2083. doi: 10.1105/tpc.113.113035

782 Campanelli, G., Sestili, S., Acciarri, N., Montemurro, F., Palma, D., Leteo, F., *et al.*
783 (2019). Multi-parental advances generation inter-cross population, to develop
784 organic tomato genotypes by participatory plant breeding. *Agronomy*, *9*, 119. doi:
785 10.3390/agronomy9030119

786 Cao, K., Cui, L., Zhou, X., Ye, L., Zou, Z., and Deng, S. (2016). Four tomato
787 *FLOWERING LOCUS T-like* proteins act antagonistically to regulate floral
788 initiation. *Front. Plant Sci.*, *6*, 1213. doi: 10.3389/fpls.2015.01213

789 Cavanagh, C., Morell, M., Mackay, I., and Powell, W. (2008). From mutations to
790 MAGIC: resources for gene discovery, validation and delivery in crop plants. *Curr.
791 Opin. Plant Biol.*, *11*, 215–221. doi: 10.1016/j.pbi.2008.01.002

792 Chen, S. (2023). Ultrafast one-pass FASTQ data preprocessing, quality control, and
793 deduplication using fastp. *iMeta*, e107. doi: 10.1002/imt2.107

794 Cingolani, P., Platts, A., Wang, L. L., Coon, M., Nguyen, T., Wang, L., *et al.* (2012). A
795 program for annotating and predicting the effects of single nucleotide
796 polymorphisms, SnpEff: SNPs in the genome of *Drosophila melanogaster* strain
797 *w1118; iso-2; iso-3. Fly*, *6*, 80–92. doi: 10.4161/fly.19695

798 Colanero, S., Perata, P., and Gonzali, S. (2018). The *atroviolacea* gene encodes an R3-
799 MYB protein repressing anthocyanin synthesis in tomato plants. *Front. Plant. Sci.*,
800 9, 830. doi: 10.3389/fpls.2018.00830

801 DePristo, M., Banks, E., Poplin, R., Garimella, K. V., Maguire, J. R., Hartl, C., *et al.*
802 (2011). A framework for variation discovery and genotyping using next generation
803 DNA sequencing data. *Nat Genet.*, 43, 491–501. doi: 10.1038/ng.806.A

804 Díez, M. J., Picó, B., and Nuez, F. (2002). Cucurbit Genetic Resources in Europe: Ad
805 Hoc Meeting held in Adana, Turkey, 19 January 2002. Rome: International Plant
806 Genetic Resources Institute.

807 Doganlar, S., Frary, A., Ku, H. M., and Tanksley, S. D. (2002). Mapping quantitative trait
808 loci in inbred backcross lines of *Lycopersicon pimpinellifolium* (LA1589). *Genome*,
809 45, 1189–1202. doi: 10.1139/g02-091

810 Eshed, Y., and Zamir, D. (1995). An Introgression Line population of *Lycopersicum
811 pennellii* in the cultivated tomato enables the identification and fine mapping of
812 yield-associated QTL. *Genetics*, 141, 1147–1162.

813 Fei, Z., Joung, J. G., Tang, X., Zheng, Y., Huang, M., Lee, J. M., *et al.* (2010). Tomato
814 functional genomics database: A comprehensive resource and analysis package for
815 tomato functional genomics. *Nucleic Acids Res.*, 39, 1156–1163. doi:
816 10.1093/nar/gkq991

817 Fei, Z., Tang, X., Alba, R., and Giovannoni, J. (2006). Tomato Expression Database
818 (TED): a suite of data presentation and analysis tools. *Nucleic Acids Res.*, 34, 766–
819 770. doi: 10.1093/nar/gkj110

820 Frary, A., and Doganlar, S. (2003). Comparative genetics of crop plant domestication
821 and evolution. *Turkish J. Agric. For.*, 27, 59–69.

822 Frary, A., Nesbitt, T. C., Frary, A., Grandillo, S., van der Knaap, E., Cong, B., *et al.*
823 (2000). fw2.2: A quantitative trait locus key to the evolution of tomato fruit size.
824 *Science*, 289, 85–88. doi: 10.1126/science.289.5476.85

825 Fulop, D., Ranjan, A., Ofner, I., Covington, M. F., Chitwood, D. H., West, D., *et al.*
826 (2016). A new advanced backcross tomato population enables high resolution leaf
827 QTL mapping and gene identification. *G3 Genes, Genomes, Genet.*, 6, 3169–3184.
828 doi: 10.1534/g3.116.030536

829 Gould, K. S. (2004). Nature's Swiss army knife: the diverse protective roles of
830 anthocyanins in leaves. *J. Biomed. Biotechnol.*, 5, 314.

831 Gramazio, P., Jaén-Molina, R., Vilanova, S., Prohens, J., Marrero, Á., Caujapé-Castells,
832 J., *et al.* (2020b). Fostering conservation via an integrated use of conventional
833 approaches and high-throughput SPET genotyping: A case study using the
834 endangered Canarian endemics *Solanum lidi* and *S. vespertilio* (Solanaceae). *Front.
835 Plant Sci.*, 11, 757. doi: 10.3389/fpls.2020.00757

836 Gramazio, P., Pereira-Dias, L., Vilanova, S., Prohens, J., Soler, S., Esteras, J., *et al.*
837 (2020a). Morphoagronomic characterization and whole-genome resequencing of
838 eight highly diverse wild and weedy *S. pimpinellifolium* and *S. lycopersicum* var.
839 *cerasiforme* accessions used for the first interspecific tomato MAGIC population.
840 *Hortic. Res.*, 7, 174. doi: 10.1038/s41438-020-00395-w

841 Gramazio, P., Yan, H., Hasing, T., Vilanova, S., Prohens, J., and Bombarely, A. (2019).
842 Whole-genome resequencing of seven eggplant (*Solanum melongena*) and one wild
843 relative (*S. incanum*) accessions provides new insights and breeding tools for
844 eggplant enhancement. *Front. Plant Sci.*, 10, 1220. doi: doi:
845 10.3389/fpls.2019.01220

846 Hochberg, Y. (1988). A sharper bonferroni procedure for multiple tests of significance.
847 *Biometrika*, 75, 800–802. doi: 10.1093/biomet/75.4.800

848 Holm, S. (1979). A simple sequentially rejective multiple test procedure. *Scand. J. Stat.*,
849 6, 65–70.

850 Honma, S. (1963). Flowering and earliness in the tomato. *J. Hered.*, 54, 212–218.

851 Horstman, A., Willemsen, V., Boutilier, K., and Heidstra, R. (2014). AINTEGUMENTA-
852 LIKE proteins: Hubs in a plethora of networks. *Trends Plant Sci.*, 19, 146–157. doi:
853 10.1016/j.tplants.2013.10.010

854 Hosmani, P. S., Flores-Gonzalez, M., Geest, H. van de, Maumus, F., Bakker, L. V.,
855 Schijlen, E., *et al.* (2019). An improved de novo assembly and annotation of the
856 tomato reference genome using single-molecule sequencing, Hi-C proximity
857 ligation and optical maps. *bioRxiv*, 767764. doi: 10.1101/767764

858 Huang, M., Liu, X., Zhou, Y., Summers, R. M., and Zhang, Z. (2019). BLINK: A package
859 for the next level of genome-wide association studies with both individuals and
860 markers in the millions. *Gigascience*, 8, 154. doi: 10.1093/gigascience/giy154

861 Jaakola, L. (2013). New insights into the regulation of anthocyanin biosynthesis in fruits.
862 *Trends Plant Sci.*, 18, 477–483. doi: 10.1016/j.tplants.2013.06.003

863 Jiménez-Gómez, J. M., Alonso-Blanco, C., Borja, A., Anastasio, G., Angosto, T., Lozano,
864 R., *et al.* (2007). Quantitative genetic analysis of flowering time in tomato. *Genome*,
865 50, 303–315. doi: 10.1139/G07-009

866 Kang, J., and Sinha, N. R. (2010). Leaflet initiation is temporally and spatially separated
867 in simple and complex tomato (*Solanum lycopersicum*) leaf mutants: A
868 developmental analysis. *Botany*, 88, 710–724. doi: 10.1139/b10-051

869 Kudo, T., Kobayashi, M., Terashima, S., Katayama, M., Ozaki, S., Kanno, M., *et al.*
870 (2017). TOMATOMICS: A web database for integrated omics information in
871 tomato. *Plant Cell Physiol.*, 58, e8(1–12). doi: 10.1093/pcp/pcw207

872 Letunic, I., and Bork, P. (2019). Interactive Tree of Life (iTOL) v4: Recent updates and
873 new developments. *Nucleic Acids Res.*, 47, 256–259. doi: 10.1093/nar/gkz239

874 Li, H. (2013). Aligning sequence reads, clone sequences and assembly contigs with
875 BWA-MEM. *arXiv* [Preprint], 1303.3997. Available at:
876 <http://arxiv.org/abs/1303.3997>

877 Lin, Z., Griffith, M. E., Li, X., Zhu, Z., Tan, L., Fu, Y., *et al.* (2007). Origin of seed
878 shattering in rice (*Oryza sativa* L.). *Planta*, 226, 11–20. doi: 10.1007/s00425-006-
879 0460-4

880 Lin, Z., Li, X., Shannon, L. M., Yeh, C. T., Wang, M. L., Bai, G., *et al.* (2012). Parallel
881 domestication of the *Shattering1* genes in cereals. *Nat. Genet.*, 44, 720–724. doi:
882 10.1038/ng.2281

883 Lippman, Z., Semel, Y., and Zamir, D. (2007). An integrated view of quantitative trait
884 variation using tomato interspecific introgression lines. *Curr. Opin. Genet. Dev.*, 17,
885 545–552. doi: 10.1016/j.gde.2007.07.007

886 Lippman, Z., and Tanksley, S. D. (2001). Dissecting the genetic pathway to extreme fruit
887 size in tomato using a cross between the small-fruited wild species *Lycopersicon*
888 *pimpinellifolium* and *L. esculentum* var. Giant Heirloom. *Genetics*, 158, 413–422.
889 doi: 10.1093/genetics/158.1.413

890 Mackay, I., and Powell, W. (2007). Methods for linkage disequilibrium mapping in crops.
891 *Trends Plant Sci.*, 12, 57–63. doi: 10.1016/j.tplants.2006.12.001

892 Mangino, G., Arrones, A., Plazas, M., Pook, T., Prohens, J., Gramazio, P., *et al.* (2022).
893 Newly developed MAGIC population allows identification of strong associations
894 and candidate genes for anthocyanin pigmentation in eggplant. *Front. Plant Sci.*, 13,
895 847789. doi: 10.3389/fpls.2022.847789

896 Martínez-Cuenca, M. R., Pereira-Dias, L., Soler, S., López-Serrano, L., Alonso, D.,
897 Calatayud, Á., *et al.* (2020). Adaptation to water and salt stresses of *Solanum*

898 *pimpinellifolium* and *Solanum lycopersicum* var. *cerasiforme*. *Agronomy*, *10*, 1169.
899 doi: 10.3390/agronomy10081169

900 Meir, Z., Aviezer, I., Chonglo, G. L., Ben-Kiki, O., Bronstein, R., Mukamel, Z., *et al.*
901 (2021). Dissection of floral transition by single-meristem transcriptomes at high
902 temporal resolution. *Nat. Plants*, *7*, 800–813. doi:10.1038/s41477-021-00936-8.

903 Muños, S., Ranc, N., Botton, E., Bérard, A., Rolland, S., Duffé, P. *et al.* (2011). Increase
904 in tomato locule number is controlled by two single-nucleotide polymorphisms
905 located near *WUSCHEL*. *Plant Physiol.*, *156*, 2244–2254. doi:
906 10.1104/pp.111.173997

907 Nakano, H., Kobayashi, N., Takahata, K., Mine, Y., and Sugiyama, N. (2016).
908 Quantitative trait loci analysis of the time of floral initiation in tomato. *Sci. Hortic.*,
909 *201*, 199–210. doi: 10.1016/j.scienta.2016.02.009

910 Nakayama, H., Ichihashi, Y., and Kimura, S. (2023). Diversity of tomato leaf form
911 provides novel insights into breeding. *Breed. Sci.*, *73*, 76–85. doi:
912 10.1270/jsbbs.22061

913 Nesbitt, T. C., and Tanksley, S. D. (2001). *fw2.2* directly affects the size of developing
914 tomato fruit, with secondary effects on fruit number and photosynthate distribution.
915 *Plant Physiol.*, *127*, 575–583. doi: 10.1104/pp.010087

916 Nesbitt, T. C., and Tanksley, S. D. (2002). Comparative sequencing in the genus
917 *Lycopersicon*: Implications for the evolution of fruit size in the domestication of
918 cultivated tomatoes. *Genetics*, *162*, 365–379. doi: 10.1093/genetics/162.1.365

919 Ofner, I., Lashbrooke, J., Pleban, T., Aharoni, A., and Zamir, D. (2016). *Solanum*
920 *pennellii* backcross inbred lines (BILs) link small genomic bins with tomato traits.
921 *Plant J.*, *87*, 151–160. doi: 10.1111/tpj.13194

922 Olsen, K. M., Slimestad, R., Lea, U. S., Brede, C., Lovald, T., Ruoff, P., *et al.* (2009).
923 Temperature and nitrogen effects on regulators and products of the flavonoid
924 pathway: Experimental and kinetic model studies. *Plant, Cell Environ.*, *32*, 286–
925 299. doi: 10.1111/j.1365-3040.2008.01920.x

926 Oróstica, K. Y., and Verdugo, R. A. (2016). Chromosome visualization tool: A whole
927 genome viewer. *Int. J. Plant Genomics*, *32*, 2366–2368. doi: 10.1155/2011/373875

928 Paran, I., Goldman, I., Tanksley, S. D., and Zamir, D. (1995). Recombinant inbred lines
929 for genetic mapping in tomato. *Theor. Appl. Genet.*, *90*, 542–548. doi:
930 10.1007/BF00222001

931 Pascual, L., Desplat, N., Huang, B. E., Desgroux, A., Bruguier, L., Bouchet, J. P., *et al.*
932 (2015). Potential of a tomato MAGIC population to decipher the genetic control of
933 quantitative traits and detect causal variants in the resequencing era. *Plant
934 Biotechnol. J.*, *13*, 565–577. doi: 10.1111/pbi.12282

935 Peralta, I. E., Spooner, D. M., Knapp, S. (2008). Taxonomy of wild tomatoes and their
936 relatives (*Solanum* Sect. *Lycopersicoides*, Sect. *Juglandifolia*, Sect. *Lycopersicon*;
937 Solanaceae). *Syst. Bot. Monogr.*, *84*, 1–186.

938 Pereira, L., Zhang, L., Sapkota, M., Ramos, A., Razifard, H., Caicedo, A. L., *et al.* (2021).
939 Unraveling the genetics of tomato fruit weight during crop domestication and
940 diversification. *Theor. Appl. Genet.*, *134*, 3363–3378. doi: 10.1007/s00122-021-
941 03902-2

942 Pin, P. A., and Nilsson, O. (2012). The multifaceted roles of *FLOWERING LOCUS T* in
943 plant development. *Plant, Cell Environ.*, *35*, 1742–1755. doi: 10.1111/j.1365-
944 3040.2012.02558.x

945 Pnueli, L., Gutfinger, T., Hareven, D., Ben-Naim, O., Ron, N., Adir, N., *et al.* (2001).
946 Tomato SP-interacting proteins define a conserved signaling system that regulates

947 shoot architecture and flowering. *Plant Cell*, 13, 2687–2702. doi:
948 10.1105/tpc.010293

949 Pook, T., Schlather, M., De Los Campos, G., Mayer, M., Carolin Schoen, C., and
950 Simianer, H. (2019). Haploblocker: Creation of subgroup-specific haplotype blocks
951 and libraries. *Genetics*, 212, 1045–1061. doi: 10.1534/genetics.119.302283

952 Price, A. L., Patterson, N. J., Plenge, R. M., Weinblatt, M. E., Shadick, N. A., and Reich,
953 D. (2006). Principal components analysis corrects for stratification in genome-wide
954 association studies. *Nat. Genet.*, 38, 904–909. doi: 10.1038/ng1847

955 Quinet, M., Bataille, G., Dobrev, P. I., Capel, C., Gómez, P., Capel, J., *et al.* (2014).
956 Transcriptional and hormonal regulation of petal and stamen development by
957 *STAMENLESS*, the tomato (*Solanum lycopersicum* L.) orthologue to the B-class
958 *APETALA3* gene. *J. Exp. Bot.*, 65, 2243–2256. doi: 10.1093/jxb/eru089

959 Reveille, W. (2017). *psych*: Procedures for personality and phychological research.
960 Northwestern University: Evanston, IL, USA.

961 Robinson, J., Thorvaldsdóttir, H., Turner, D., and Mesirov, J. (2023). igv.js: an
962 embeddable JavaScript implementation of the Integrative Genomics Viewer (IGV).
963 *Bioinformatics*, 39, btac830. doi: 10.1093/bioinformatics/btac830

964 Rothan, C., Diouf, I., and Causse, M. (2019). Trait discovery and editing in tomato. *Plant
965 J.*, 97, 73–90. doi: 10.1111/tpj.14152

966 Saitou, N., and Nei, M. (1987). The neighbor-joining method: a new method for
967 reconstructing phylogenetic trees. *Mol. Biol. Evol.*, 4, 406–425. doi:
968 10.1093/oxfordjournals.molbev.a040454

969 Salinas, M., Capel, C., Alba, J. M., Mora, B., Cuartero, J., Fernández-Muñoz, R., *et al.*
970 (2013). Genetic mapping of two QTL from the wild tomato *Solanum
971 pimpinellifolium* L. controlling resistance against two-spotted spider mite
972 (*Tetranychus urticae* Koch). *Theor. Appl. Genet.*, 126, 83–92. doi: 10.1007/s00122-
973 012-1961-0

974 Scott, M. F., Ladejobi, O., Amer, S., Bentley, A. R., Biernaskie, J., Boden, S. A., *et al.*
975 (2020). Multi-parent populations in crops: a toolbox integrating genomics and
976 genetic mapping with breeding. *Heredity*, 125, 396–416. doi: 10.1038/s41437-020-
977 0336-6

978 Semel, Y., Nissenbaum, J., Menda, N., and Zamir, D. (2006). Overdominant quantitative
979 trait loci for yield and fitness in tomato. *Proc. Natl. Acad. Sci.*, 103, 12981–12986.
980 doi: 10.1073/pnas.0604635103

981 Shani, E., Burko, Y., Ben-Yaakov, L., Berger, Y., Amsellem, Z., Goldshmidt, A., *et al.*
982 (2009). Stage-specific regulation of *Solanum lycopersicum* leaf maturation by class
983 1 KNOTTED1-LIKE HOMEOBOX Proteins. *Plant Cell*, 21, 3078–3092. doi:
984 10.1105/tpc.109.068148

985 Shwartz, I., Levy, M., Ori, N., and Bar, M. (2016). Hormones in tomato leaf development.
986 *Dev. Biol.*, 419, 132–142. doi: 10.1016/j.ydbio.2016.06.023

987 Silva, G. F. F., Silva, E. M., Correa, J. P. O., Vicente, M. H., Jiang, N., Notini, M. M., *et
988 al.* (2019). Tomato floral induction and flower development are orchestrated by the
989 interplay between gibberellin and two unrelated microRNA-controlled modules.
990 *New Phytol.*, 221, 1328–1344. doi: 10.1111/nph.15492

991 Snouffer, A., Kraus, C., and van der Knaap, E. (2020). The shape of things to come: ovate
992 family proteins regulate plant organ shape. *Curr. Opin. Plant Biol.*, 53, 98–105. doi:
993 10.1016/j.pbi.2019.10.005

994 Suresh, B. V., Roy, R., Sahu, K., Misra, G., and Chattopadhyay, D. (2014). Tomato
995 genomic resources database: An integrated repository of useful tomato genomic

996 information for basic and applied research. *PLoS One*, 9, e86387. doi:
997 10.1371/journal.pone.0086387

998 Szymkowiak, E. J., and Irish, E. E. (2006). *JOINTLESS* suppresses sympodial identity in
999 inflorescence meristems of tomato. *Planta*, 223, 646–658. doi: 10.1007/s00425-005-
1000 0115-x

1001 Tanksley, S. D., and Nelson, J. C. (1996). Advanced backcross QTL analysis: A method
1002 for the simultaneous discovery and transfer of valuable QTLs from unadapted
1003 germplasm into elite breeding lines. *Theor. Appl. Genet.*, 92, 191–203. doi:
1004 10.1007/BF00223376

1005 Thissen, D., Steinberg, L., and Kuang, D. (2002). Quick and easy implementation of the
1006 Benjamini-Hochberg procedure for controlling the false positive rate in multiple
1007 comparisons. *J. Educ. Behav. Stat.*, 27, 77–83. doi: 10.3102/10769986027001077

1008 Troyanskaya, O., Cantor, M., Sherlock, G., Brown, P., Hastie, T., Tibshirani, R., *et al.*
1009 (2001). Missing value estimation methods for DNA microarrays. *Bioinformatics*, 17,
1010 520–525. doi: 10.1093/bioinformatics/17.6.520

1011 Turck, F., Fornara, F., and Coupland, G. (2008). Regulation and identity of florigen:
1012 *Flowering Locus T* moves center stage. *Annu. Rev. Plant Biol.*, 59, 573–594. doi:
1013 10.1146/annurev.arplant.59.032607.092755

1014 Ueta, R., Abe, C., Watanabe, T., Sugano, S. S., Ishihara, R., Ezura, H., *et al.* (2017).
1015 Rapid breeding of parthenocarpic tomato plants using CRISPR/Cas9. *Sci. Rep.*, 7,
1016 507. doi: 10.1038/s41598-017-00501-4

1017 van der Knaap, E., Chakrabarti, M., Chu, Y. H., Clevenger, J. P., Illa-Berenguer, E.,
1018 Huang, Z., *et al.* (2014). What lies beyond the eye: The molecular mechanisms
1019 regulating tomato fruit weight and shape. *Front. Plant Sci.*, 5, 227. doi:
1020 10.3389/fpls.2014.00227

1021 Vilanova, S., Alonso, D., Gramazio, P., García-Fortea, E., Ferrante, P., Schmidt, M., *et*
1022 *al.* (2020). SILEX: A fast and inexpensive high-quality DNA extraction method
1023 suitable for multiple sequencing platforms and recalcitrant plant species. *Plant
1024 Methods*, 16, 1–11. doi: 10.1186/s13007-020-00652-y

1025 Wang, J., and Zhang, Z. (2021). GAPIT version 3: boosting power and accuracy for
1026 genomic association and prediction. *Genomics, Proteomics Bioinforma.*, 19, 629–
1027 640. doi: 10.1016/j.gpb.2021.08.005

1028 Wang, S., Chang, Y., and Ellis, B. (2016). Overview of OVATE FAMILY PROTEINS,
1029 a novel class of plant-specific growth regulators. *Front. Plant Sci.*, 7, 417. doi:
1030 10.3389/fpls.2016.00417

1031 Wei, T., and Simko, V. (2017). R Package “Corrplot”: Visualization of a Correlation
1032 Matrix. R Core Team: Vienna, Austria.

1033 Wickham, H. (2009). ggplot2: Elegant graphics for data analysis. *Media*, 35, 10–1007.

1034 Yu, J., Pressoir, G., Briggs, W. H., Bi, I. V., Yamasaki, M., Doebley, J. F., *et al.* (2006).
1035 A unified mixed-model method for association mapping that accounts for multiple
1036 levels of relatedness. *Nat. Genet.*, 38, 203–208. doi: 10.1038/ng1702

1037 Zhang, D., Ai, G., Ji, K., Huang, R., Chen, C., Yang, Z., *et al.* (2023). *EARLY
1038 FLOWERING* is a dominant gain-of-function allele of *FANTASTIC FOUR* *I/2c* that
1039 promotes early flowering in tomato. *Plant Biotechnol. J.* doi: 10.1111/pbi.14217

1040 Zhang, J., Chen, R., Xiao, J., Qian, C., Wang, T., Li, H., *et al.* (2007). A single-base
1041 deletion mutation in *SlIAA9* gene causes tomato (*Solanum lycopersicum*) *entire*
1042 mutant. *J. Plant Res.*, 120, 671–678. doi: 10.1007/s10265-007-0109-9

1043 Zhang, R., Jia, G., and Diao, X. (2023). geneHapR: an R package for gene haplotypic
1044 statistics and visualization. *BMC Bioinformatics*, 24, 199. doi: 10.1186/s12859-023-
1045 05318-9

Zhang, Y., Butelli, E., and Martin, C. (2014). Engineering anthocyanin biosynthesis in plants. *Curr. Opin. Plant Biol.*, 19, 81–90. doi: 10.1016/j.pbi.2014.05.011

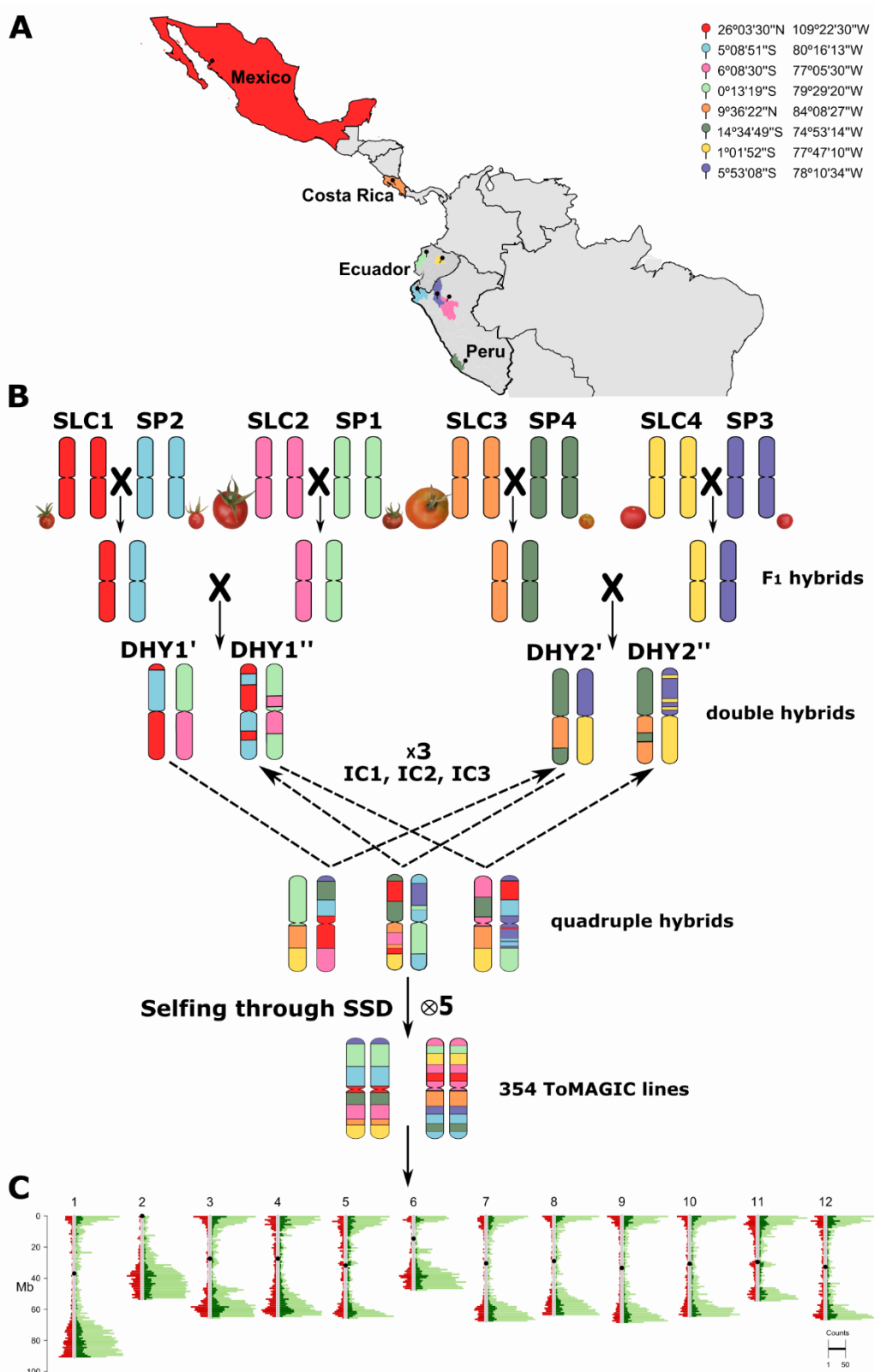


Figure 1. (A) Origin of the different SLC and SP founders selected for the ToMAGIC population development represented with the different colours code. (B) The funnel breeding design to develop the 354 ToMAGIC lines. The eight founders with a different colour to represent their genomic background, are represented at a scale based on the real fruit size. (C) Distribution of the 6,488 filtered markers (in red), the Heinz 1706 SL4.0 annotated genes (in light green), and the genes covered by the filtered markers (in dark green) across the 12 tomato chromosomes.

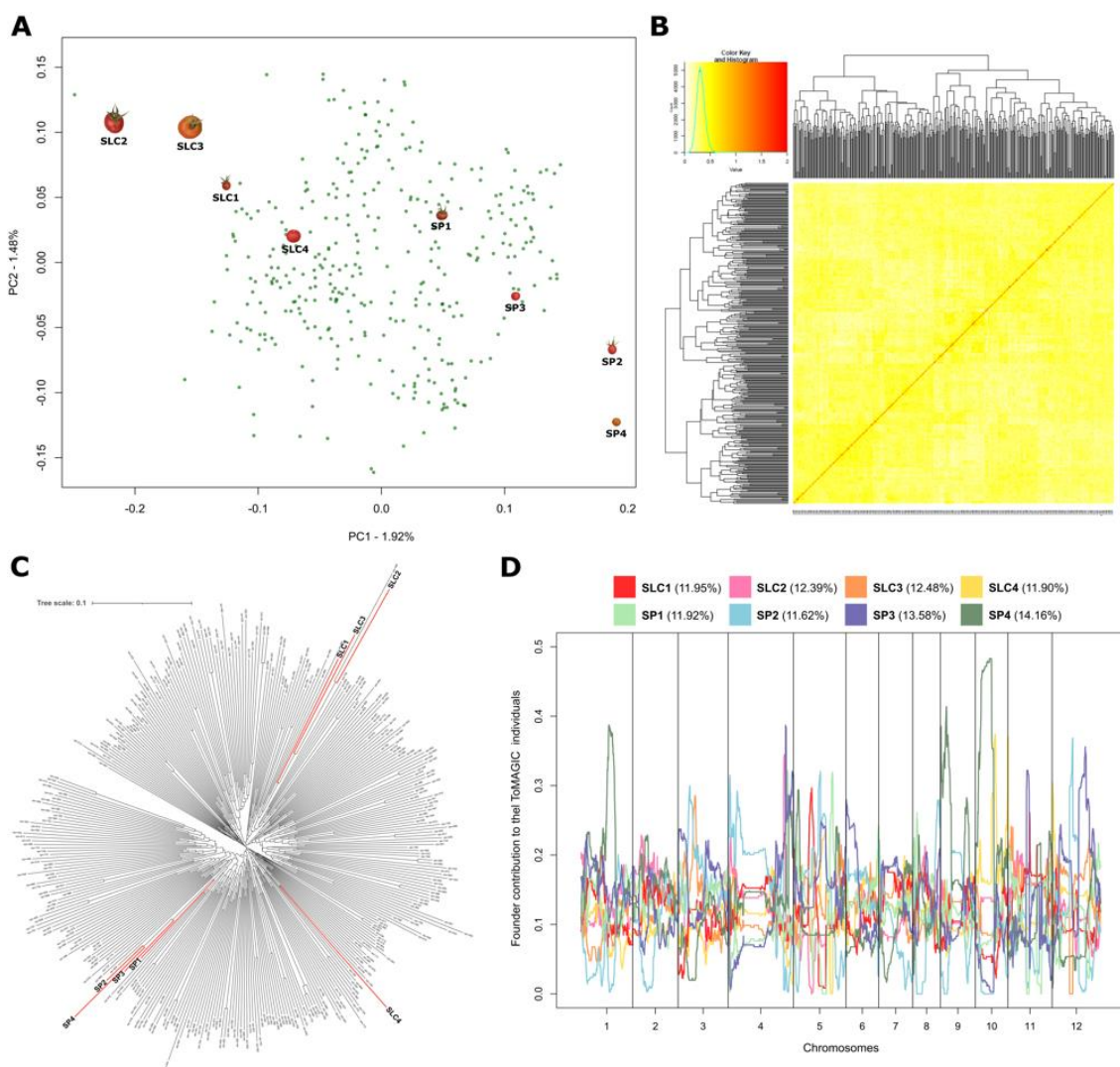


Figure 2. Population structure of the inter-specific ToMAGIC population. (A) Principal component analysis (PCA) plot of the first two PCs. (B) Heatmap plot of genetic relationship based on the kinship matrix. (C) Dendrogram indicating founders' locations with coloured red branches. (D) Genome-wide founder haplotype blocks assignment across the 12 tomato chromosomes (x-axis) as the average percentage of founders' contribution to the ToMAGIC lines (y-axis) with a different colour associated with each founder.

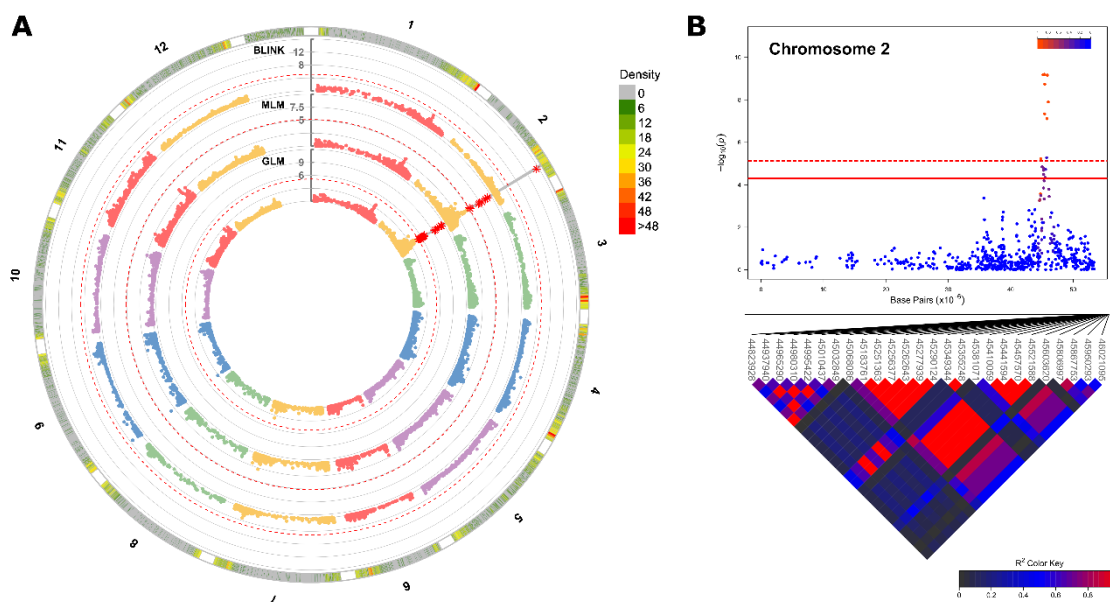


Figure 3. Genome-wide association results for the locule number trait. (A) Manhattan plots comparing GLM, MLM and BLINK models. The solid grey line indicates the common significant markers detected by two or more models. The red asterisks indicate the SNPs exceeding the Bonferroni threshold, represented as a dashed red line. (B) On the top, a chromosome-wise Manhattan plot with the top significant markers. Bonferroni and FDR thresholds are represented with red dashed and continuous lines, respectively. The colour from blue to red indicates r^2 from 0 to 1. On the bottom, heat map of pairwise linkage disequilibrium (LD). SNP positions under the significant region are indicated in bp. The colour from black to red indicates r^2 from 0 to 1.

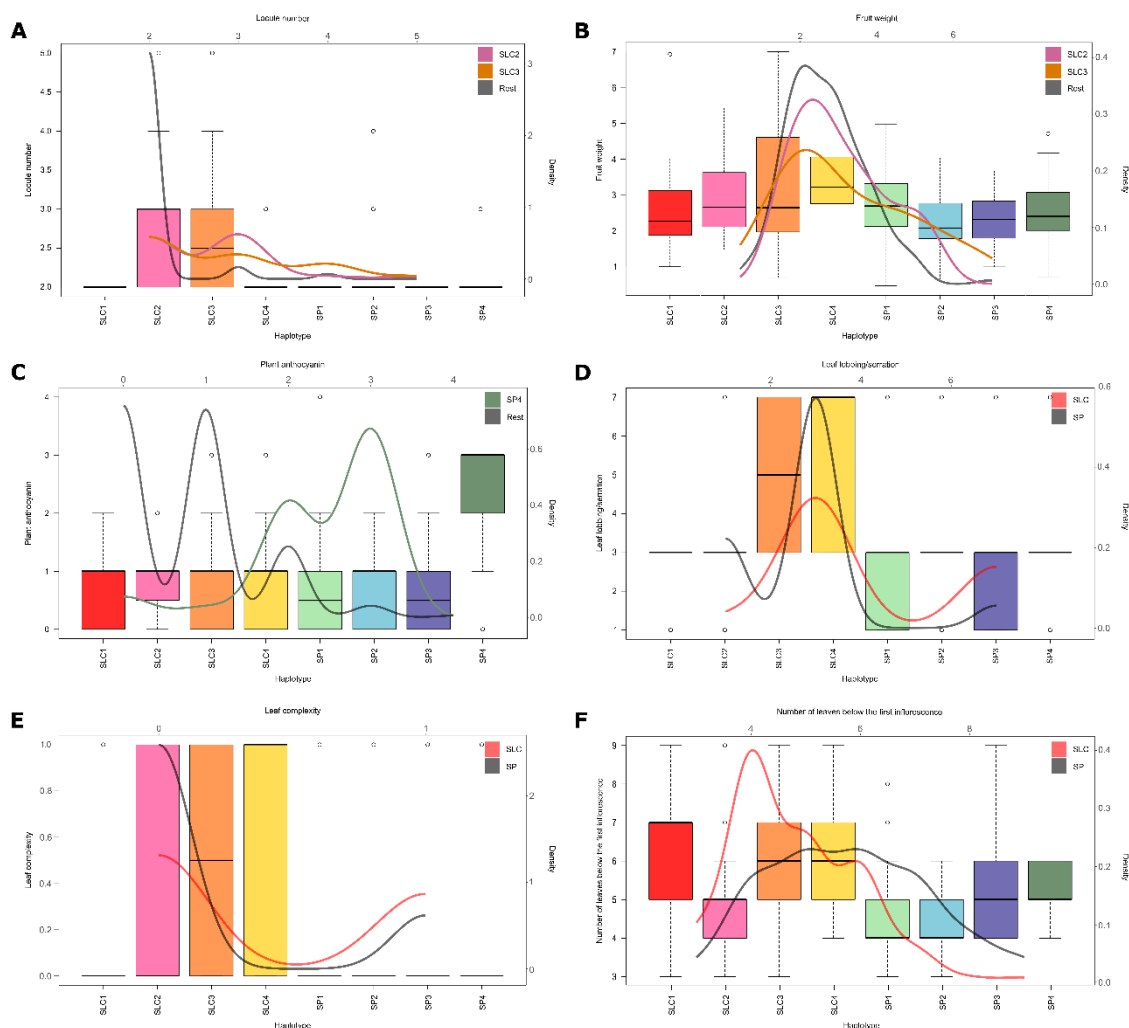


Figure 4. Haplotype analysis of the ToMAGIC lines for each of the MAGIC founders' haplotype in combination with phenotypic data. Boxplot and density plot distribution in the candidate genomic regions for: (A) locule number; (B) fruit weight; (C) plant anthocyanin on chromosome 7; (D) leaf lobing/serration; (E) leaf complexity; and (F) number of leaves below the first inflorescence.